To the University of Wyoming:

The members of the Committee approve the thesis of Yifan Zhang presented on 11/18/2014.

Ye Zhang, Chairperson

Thijs J. Kelleners, External Department Member

Subhashis Mallick

APPROVED:

Paul Heller, Department Chair, Department of Geology and Geophysics.

Paula M. Lutz, College Dean, College of Arts and Sciences

ABSTRACT

Zhang, Yifan, MS in Geology, Department of Geology & Geophysics, Dec, 2014

A physics-based inverse method is proposed for simultaneous parameter, boundary condition, and flow fields (which includes hydraulic head field, Darcy flux fields, and streamlines) estimation for a discrete fractured aquifer. By sampling synthetic aquifer problems (i.e., forward models) containing various fracture patterns to provide observation data for inversion, the inverse method is tested for parameter estimation under varying observation data quality, data density, and the ratio of fracture conductivity (K_f) to matrix conductivity (K_m). This method can achieve stable parameter estimations for measurement errors up to +/- 10% of the total hydraulic head variation of the forward model. But the accuracy of parameter estimation is sensitive to data density. In addition, hydraulic heads, Darcy fluxes, streamlines, and boundary conditions are also recovered by inversion and are found to capture the major characteristics of the flow field. The scientific importance of recovering boundary conditions by inversion is also verified by running a set of test problems with PEST and comparing its solutions with those obtained with the direct method. Furthermore, effective hydraulic conductivity to represent flow in a fractured aquifer is also successfully estimated by inverse method.

PHYSICS-BASED GROUNDWATER INVERSION OF FRACTURED AQUIFERS WITH UNKNOWN BOUNDARY CONDITIONS

By

Yifan Zhang

A thesis submitted to the Department of Geology & Geophysics

and the University of Wyoming

in partial fulfillment of the requirements

for the degree of Master of Science

MASTER OF SCIENCE

in

GEOLOGY

Laramie, Wyoming

December 2014

ACNOWLEDGEMENTS

First and foremost, I would like to express my sincere gratitude to my advisor Prof. Ye Zhang for her guidance, patience, enthusiasm, encouragement, and continuous support for my study and research.

Besides my advisor, I would like to thank the rest of my thesis committee: Prof. Subhashis Mallick and Prof. Thijs J. Kelleners for their time and insightful comments.

Finally, I wish to give special thanks to my parents and sister for their love and support.

Contents

LIST OF FIGURES

LIST OF TABLES

CHAPTER 1   INTRODUCTION

Fractures are defined as "displacement discontinuities in rocks, which appear as local breaks in the natural sequence of the rock's properties" (Tiab & Donaldson, 2011). They are discontinuities where minerals and rocks are broken. Fractures can be characterized as reduction or loss of cohesion in most cases (Fossen, 2010). They are formed when the stress in rocks exceeds a certain limit, and thus the rocks fail mechanically. Natural fractures range on a scale from micro-cracks to crustal rifts (Bonnet et al., 2001). Normally fractures are preferential flow paths, but when less permeable material is contained in fractures, fractures may form flow barriers.

Fractured geological formations exist almost everywhere in the world (Berkowitz, 2002). Although fractures only make up a small percent of the volume of the entire formation, they have a major influence on the formation's properties. The properties influenced by fractures most significantly are porosity and permeability, which are the key parameters controlling the flow performance in water and hydrocarbon reservoir production. Characterizing fractured formations is one of the most challenging tasks for hydrologists and production geologists (Faybishenko, Witherspoon, & Benson, 2000).

During the history of sedimentary process, nearly all sedimentary formations in the upper part of the earth's crust have been fractured to some extent. As a result, the definition of "fractured reservoir" does not rely on the presence of fractures, but depends on the influence of fractures on fluid flow behavior (Bourbiaux, 2010). By this definition, it is estimated that 20% of world oil

reserves lies in fractured reservoirs (Abbas, 2000). Other people have estimated that 40% of world's oil reserves are contained in carbonate formations, which are highly likely fractured (Perrodon, 1980). Even when production is performed in un-fractured formations, artificial fractures (e.g. hydraulic fractures) may be generated to enhance production.

Naturally fractured reservoirs are the most complicated water and hydrocarbon reserves. To reveal how natural fractures impact reservoir performance, fluid flow modeling and reservoir simulation is widely applied and investigated. Reservoir simulation can be performed to optimize water and hydrocarbon recovery, to calculate economic worth of a reservoir, and to evaluate the risk (Lemonnier & Bourbiaux, 2010). As a result, reservoir simulation is a crucial tool for reservoir management.

Past works have proven that models that treat fractured formations as uniform or non-uniform isotropic continuum usually cannot always predict flow and transport in those formations successfully. Instead, models must honor the heterogeneity of fractured rocks. One method is to represent the rock by a discreet fracture network, and the other is to depict the rock as a stochastic medium (Shlomo P. Neuman, 2005). In this thesis, the discreet fracture method is applied as every single fracture is assumed to be known by its location, shape, size, and orientation.

The heterogeneities of fractured aquifers may range across multiple scales (Bonnet et al., 2001). To test the performance of the physics-based inverse method under multiple scales of heterogeneity, parameters are estimated when the ratio between fracture conductivity (K_f) and matrix conductivity (K_m) ranges from ten to a million. On the other hand, flow generally takes place in preferential flow paths in fractured formations (Tsang & Neretnieks, 1998). To

investigate the significance of the preferential flow paths, streamlines are generated using inversed conductivities and boundary conditions (BC) to compare to the true streamlines.

This thesis performs model calibrations with observation data of hydraulic heads and Darcy flux vectors to estimate hydraulic conductivities. Hydraulic heads are easy to measure in wells, while Darcy flux can be tested by a point velocity probe (PVP) which is a new tool and can be used to measure groundwater velocities at the centimeters scale (Labaky, Devlin, & Gillham, 2009). Darcy flux can also be calculated from direct flow rate measurements, which can also be obtained in the field (Bayless, Mandell, & Ursic, 2011; Devlin et al., 2012). The hydraulic conductivity can be inverted if the observation data provided are sufficiently sensitive to the property of interest (Kowalsky et al., 2012). However, observation data can be expensive to obtain and thus measurements available are very limited. Calibration of groundwater models without enough measurements is an underdetermined inverse problem (Mclaughlin & Townley, 1996). To overcome this problem, a common method is to make simplifying assumptions regarding spatial variability (Moore & Doherty, 2006). In this thesis, deterministic models are defined where the exact spatial distribution of hydraulic conductivities is known and the nonuniqueness problem is avoided.

In most parameter estimation studies, the focus point has been on the indirect inverse method solving a boundary value problem to optimize an objective function, which aims to minimize the measurement-to-model misfits. In these methods, the hydrologic properties of heterogeneous formations are inverted starting with an initial guess of parameter values and boundary conditions. Then observation data of hydraulic heads and flow rates are compared to the corresponding simulation results obtained by running the forward mathematical model. The

parameters (sometimes also the boundary conditions) of the mathematical model are adjusted after each simulation until a satisfactory match to the observation data is obtained, or the value of the objective function is minimized. The final parameter values are considered as a reasonable representation of the geologic formation (Doughty, Long, Hestir, & Benson, 1994). Such approaches satisfy the known physics and mathematical constraints, are easily adaptable, and have proven to be robust and efficient in many situations. But they require the assumption of boundary conditions which are usually unknown and will cause great uncertainty. Also parameter estimation via those indirect methods are often an iterative procedure involving repeated simulations of the boundary value problem as stated before, which is a computationally intense task especially when the model size is large. On the other hand, even though both parameters (hydraulic conductivities) and boundary conditions can be modified and updated by iterations, the inverse problem can be ill posed, e.g., instability, nonuniqueness, and failure to converge could happen. Furthermore, an infinite number of boundary conditions may fit the observation data equally well; thus the inferred boundary conditions are generally non-unique.

Direct methods can also be used to solve the inverse problems. The direct methods are mathematically straightforward and computationally efficient. However, the direct methods have not been widely adopted due to their instability of the estimated parameters when the observation data contains error. In hydrogeology, initial attempts were made to directly determine transmissibility from streamlines by inverting the flow equation along these lines, but this method was found sensitive to measurement errors and thus cannot obtain reliable parameter estimation (Nelson, 1960, 1961, 1968). Though parameter uncertainty can be controlled by imposing bounds on the observation errors (Kleinecke, 1971), solutions are often unreliable. Other direct methods such as the direct matrix method create a set of superdeterminate algebraic

equations from discretizing the boundary value problem (S. P. Neuman, 1973; Sagar, Yakowitz, & Duckstein, 1975). In a two-dimensional problem, when random noise is added to the observation data, the direct matrix method is found accurate when the parameter dimension is small (Yeh, Yoon, & Lee, 1983). Sun (Sun, 1994) stated that the necessary condition for parameter identifiability is that the number of parameters is smaller than the number of observation data.

This thesis tests the liability of the physics-based direct method for parameter estimation. This method does not require the presumption of boundary conditions; instead it can recover boundary conditions by inversion along with the hydraulic parameters. This method is mathematically straightforward and computationally efficient. It discretizes the problem domain into elements and state variables are approximated by a function satisfying the governing equation, the Laplace's equation. State variables at the observation points are then directly incorporated. The unknown hydraulic conductivity is estimated together with parameters in the head and flux functions. To ensure head and flux continuity at element boundaries, a collocation technique is used; elements within one hydro face assume continuous heads and fluxes in all directions, while elements separated by a material interface assume continuity in head and continuity of the normal flux. The inversion problem is thus stated with correct physical constraints. Using Laplace's solution with unknown coefficients, the method in effect estimates the coefficients by "bending" the approximate solution toward the true solution, following the observations with their weights. Unlike the existing indirect and direct methods, this method does not discretize a boundary value problem; thus a priori knowledge of the boundary condition is not required. Also this method does not attempt to fit boundary conditions to observation data, avoiding the nonuniqueness problem. In a single step (i.e., single matrix solve), model

parameters and model state variables are simultaneously estimated, and boundary conditions of the modeling region can be inferred by the inverted hydraulic heads along the boundary (Irsa & Zhang, 2012).

In this thesis, steady state groundwater flow in heterogeneous isotropic confined aquifers characterized by fractures and flow barriers are investigated by the physics-based direct inverse method.

CHAPTER 2   BACKGROUND

1.   **Nonuniqueness in Fitting Boundary Conditions to a Steady State Problem**

Most existing methods utilize the solution of a boundary value problem with prescribed boundary conditions which can be modified and updated during inversion, along with the parameters of the model. The main issue of these methods is that the fitted boundary conditions are not unique. The other issue of these methods is that they are computationally intensive as numerous forward simulations are involved until a good fit between the forward simulation results and the observation data is obtained.

The severity of the nonuniqueness depends on the quantity and quality of the observation data. When enough data is available and the data quality is high, the nonuniqueness is less pronounced. But even in this case, there still exists more than one set of boundary conditions providing solutions that satisfy the observed data and prior information. On the other hand, it is commonly assumed that by adding flow rate data, the nonuniqueness in fitting the hydraulic heads can be reduced and perhaps a unique solution is possible because a flow rate measured at any point in the aquifer would impose an additional constraint on the solution. However, the addition of flow rate data does not guarantee a unique solution.

The nonuniqueness issue can be demonstrated by a two-dimensional example of steady state groundwater flow in a homogeneous isotropic aquifer (Irsa & Zhang, 2012). In this example, the hydraulic heads satisfy the Laplace's equation. Figure 2.1(a) shows that 3 hydraulic heads are sampled in the study domain, with two located at the corners on the left and the other one located at the middle of the right boundary. In addition, a flow rate is also obtained analytically along the

y axis on the right boundary. Figure 2.1(b) shows that two different sets of boundary conditions are specified along the study domain. Both boundary conditions honor the observation data of 3 hydraulic heads and 1 flow rate. However, these 2 different sets of boundary conditions lead to totally different reconstructed flow fields as shown by Figure 2.1(c) and Figure 2.1(d). The smoother boundary condition represented by the red line in Figure 2.1(b) leads to the smoother flow field in Figure 2.1(c). On the other hand, the more fluctuated boundary condition represented by the green line in Figure 2.1(b) leads to the less smooth flow field in Figure 2.1(d). In this example, the observation data of 3 hydraulic heads and 1 flow rate do not lead to a unique estimation of hydraulic heads along the same boundary. This example shows that the methods involving the solution of a boundary value problem with assumed boundary conditions cannot obtain unique estimation of flow fields as more than one set of boundary conditions will satisfy the same observation data. This issue is one of the major concerns with current inversion methods. Even though a unique estimation of hydraulic conductivity can be achieved, extremely different flow fields will be obtained due to different presumed boundary conditions. As a result, a great amount of uncertainty will be caused in the following prediction analysis.
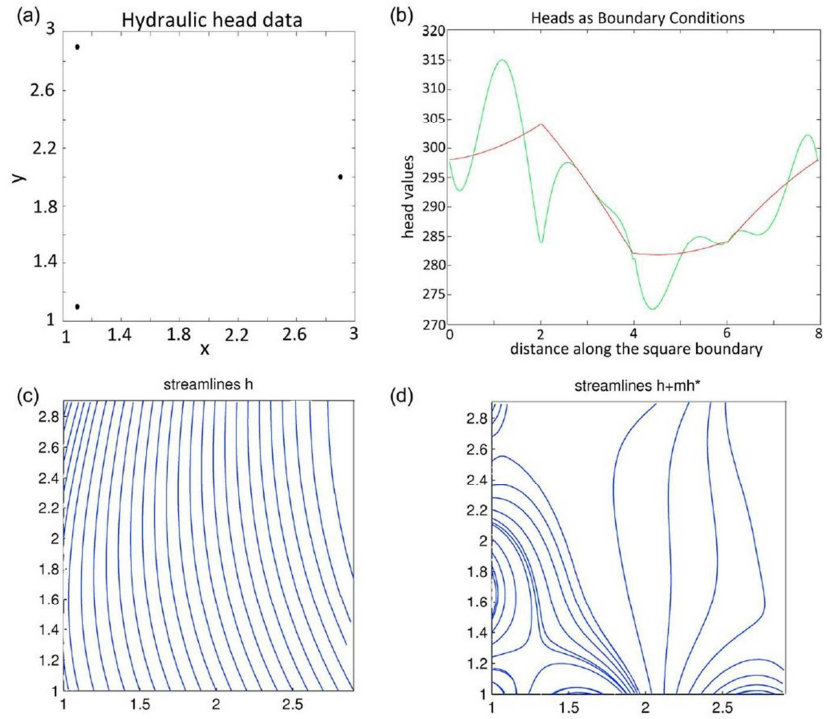
Figure 2.1: Nonuniqueness in Fitting Boundary Condition in
a 2-Dimensional Homogeneous and Isotropic Aquifer

CHAPTER 3 METHODOLOGY

1. Flow Equations

The physics-based inverse method presented below is not based on solving a boundary value problem. As a result, it does not require the presumption of boundary conditions and does not involve iteration. This method can provide the best fit to the observation data with stable convergence.

The 3-dimensional groundwater flow equation in a confined aquifer with source/sink effects is written as:

$$\frac{\partial}{\partial x}\left(K_x \frac{\partial h}{\partial x}\right) + \frac{\partial}{\partial y}\left(K_y \frac{\partial h}{\partial y}\right) + \frac{\partial}{\partial z}\left(K_z \frac{\partial h}{\partial z}\right) = S_s \frac{\partial h}{\partial t} \tag{1}$$

Where $h(x,y,z)$ is hydraulic head [L], K represents hydraulic conductivity [L/T], $S_s \frac{\partial h}{\partial t}$ is the source/sink term [L/T].

When the formation is homogeneous, K_x, K_y and K_z do not vary with space, and the flow equation can be simplified as:

$$K_x \frac{\partial^2 h}{\partial x^2} + K_y \frac{\partial^2 h}{\partial y^2} + K_z \frac{\partial^2 h}{\partial z^2} = S_s \frac{\partial h}{\partial t} \tag{2}$$

Furthermore, if the formation is isotropic which means that hydraulic conductivities in all directions are the same ($K_x = K_y = K_z = K$), then the flow equation can be simplified as:

$$\frac{\partial^2 h}{\partial x^2} + \frac{\partial^2 h}{\partial y^2} + \frac{\partial^2 h}{\partial z^2} = \frac{S_s}{K} \frac{\partial h}{\partial t} \tag{3}$$

Under the condition of homogeneous and isotropic formations, if the flow is steady state which means that the hydraulic heads do not vary with time ($\frac{\partial h}{\partial t} = 0$), then the flow equation can be further simplified as:

$$\frac{\partial^2 h}{\partial x^2} + \frac{\partial^2 h}{\partial y^2} + \frac{\partial^2 h}{\partial z^2} = 0 \tag{4}$$

At last, the 2-dimensional steady-state flow equation of a homogeneous and isotropic aquifer is:

$$\frac{\partial^2 h}{\partial x^2} + \frac{\partial^2 h}{\partial z^2} = 0 \tag{5}$$

Equation (5) is commonly known as the Laplace's equation. In this thesis, steady-state groundwater flow in homogeneous and isotropic aquifers, which is governed by the Laplace's equation, is investigated.

2. Physics-Based Inverse Method

The physics-based inversion method applied in this thesis study enforces two constraints: (1) global continuity of hydraulic heads and Darcy fluxes throughout the solution domain; (2) local conditioning of the inverse solution to observed hydraulic heads, fluxes, and flow rates (i.e., state variables) if available.

For each grid cell within the study domain, the hydraulic head (h) can be represented by a second order polynomial which satisfies the Laplace's equation:

$$h(x, z) = a_0 + a_1 x + a_2 z + a_3 xz + a_4 (x^2 - z^2) \tag{6a}$$

In this approximation, x and z are coordinates of the middle point of the grid cell; $a_0, a_1, a_2, a_3,$ and a_4 are unknown parameters of the grid cell. With this approximation, Darcy fluxes can be obtained by differentiating hydraulic heads:

$$q_x(x,z) = -K^e \frac{\partial h}{\partial x} = -K^e(a_1^e + a_3^e z + 2a_4^e x) \tag{6b}$$

$$q_z(x,z) = -K^e \frac{\partial h}{\partial z} = -K^e(a_2^e + a_3^e x - 2a_4^e z) \tag{6c}$$

In the equations, K^e represents the hydraulic conductivity of the corresponding element. With the fundamental solutions described for each grid cell (equation (6)), the solution must also satisfy the governing equation globally. This is accomplished by minimizing a residual function on the collocation points. The collocation technique is used to guarantee global continuity of hydraulic heads and Darcy fluxes. Two collocation points are assigned on every boundary between grid cells (Figure 3.1). Grid cells within one hydro-face (the two grid cells on both sides of the boundary have the same hydraulic conductivity) assume continuous hydraulic heads and fluxes in all directions, while grid cells separated by a material interface (the two grid cells on each side of the boundary have different hydraulic conductivities) assume continuity in hydraulic head and continuity of the normal flux (the flux whose direction is perpendicular to the material interface). The inversion problem is thus stated with correct physical constraints. As described in Figure 3.1, the left and right boundaries are no-flow boundaries, thus there only exists vertical flow in this case.
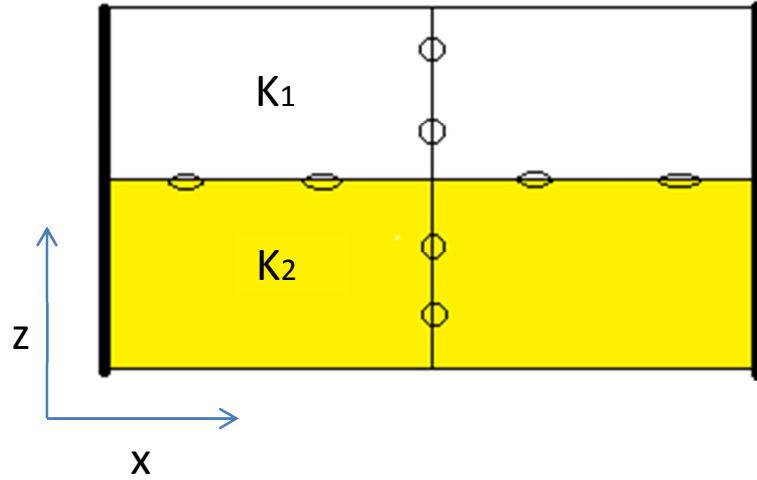
Figure 3.1:
The Sampling
Strategy of
Collocation
Points

The continuity equations at interfaces that separate different materials are:

$$\delta_{cp}^{head}\left(K_e h_{cp}^1 - K_e h_{cp}^2\right) = 0 \tag{7a}$$

$$\delta_{cp}^{q_x}\left(q_{x\,cp}^{1} - q_{x\,cp}^{2}\right) = 0 \tag{7b}$$

$$\delta_{cp}^{q_z}\left(q_{z\,cp}^{1} - q_{z\,cp}^{2}\right) = 0 \tag{7c}$$

The continuity equations at interfaces that have same hydraulic conductivity values (K) on both sides of the interface are:

$$\delta_{cp}^{head}\left(K_e h_{cp}^1 - K_e h_{cp}^2\right) = 0 \tag{8a}$$

$$\delta_{cp}^{q_z}\left(q_{z\,cp}^{1} - q_{z\,cp}^{2}\right) = 0 \tag{8b}$$

Where δ is a weighting function assigned to the equations to reflect the magnitude of the measurement errors.

The local conditioning equations (data equations) that constrain the inverse solution to observed hydraulic heads and fluxes are:

13

$$\delta^{head}\left(K_e h_{approximated} - K_e h_{observed}\right) = 0 \qquad (9a)$$

$$\delta^{flux}\left(q_{y\,approximated} - q_{y\,observed}\right) = 0 \qquad (9b)$$

Equations (7), (8), and (9) together form a matrix-vector problem, which can be solved to obtain hydraulic conductivity (K) value and all the parameter a values. With equations (6a), (6b) and (6c), the hydraulic head and Darcy flux vector of each grid cell can be determined by the $a_0, a_1, a_2, a_3,$ and a_4 values.

3. Advantages of the Physics-Based Inverse Method

This physics-based inverse method has several advantages: (1) model fits the data directly and there is no need to fit an objective function so no computationally intensive iteration is involved; (2) numerical discretization is the only source of error besides measurement error; (3) this method can uniquely determine the hydraulic heads, flow fields, as well as the boundary conditions, given observed hydraulic heads and Darcy flux data.

CHAPTER 4   RESULTS & DISCUSSIONS

The physics-based inverse method described is applied to simultaneously estimate hydraulic conductivities and boundary conditions of 2-dimensional fractured confined aquifers under steady state. Computational experiments are performed for 9 models. Groundwater in each model flows through fractures (or flow barriers) and matrix.

1. Parameter Estimation

Five forward models are constructed for 2-dimensional confined aquifers with different fracture orientations. Hydraulic conductivities of these models are estimated by inversion with observation data of hydraulic heads and Darcy fluxes. Workflow of the parameter estimation process is described as below:

1. Forward models are built in GW Vista (Version 6.25), which is a software package for groundwater flow modeling, calibration, and optimization. The software utilizes the MODFLOW suite of codes. The grid density of all 5 models is 25 by 25 (25 grid cells on both x and z directions). For MODEL 1 to MODEL 4, the top boundaries are defined as constant head boundaries with hydraulic heads equal to 600 ft; the bottom boundaries are defined as constant head boundaries with hydraulic heads equal to 500 ft; the left and right boundaries are no flow boundaries. On the other hand, for MODEL 5, the left boundary is defined as a constant head boundary of 600 ft; the right boundary is defined as a constant head boundary of 500 ft; the top and bottom boundaries are defined as no flow boundaries.

2. After running each forward model with GW Vista, the hydraulic heads at every grid cell are calculated and obtained.

3. Darcy fluxes are calculated for every grid cell by Darcy's Law (Equation 6b and 6c).

4. Hydraulic heads and Darcy flux vectors (Darcy flux components in both x and z directions) are sampled as observation data for inversion in each case.

5. Hydraulic conductivity is estimated for each model with the sampled hydraulic heads and Darcy fluxes as observation data. The inversions are performed with source code written in Matlab. The code is constructed according to the physics-based method.

For MODEL 1 to MODEL 4 (Fig 4.1 to Fig 4.4), the same sampling density is applied. The figures also show locations where observation data is sampled. The "×" symbol represents locations where hydraulic heads are sampled, and the "*" symbol represents locations where Darcy fluxes are sampled (Fig 4.4 does not show the data sampling locations, but the sampling strategy is the same as MODEL 2 shown in Fig 4.2). The K_f/K_m ratio is fixed at 10 for MODEL 1 to MODEL 4. MODEL 1 contains a single vertical fracture; MODEL 2 contains a single horizontal fracture; MODEL 3 has a vertical and a horizontal fracture; and MODEL 4 is the same as MODEL 3, except that the fracture volume is 25 times greater. The parameter estimation results of these 4 models are summarized in Table 4.1. In these 4 models, the biggest inversion error is 5.29% in MODEL 3. For MODEL 1, the inversion achieves almost perfect hydraulic conductivity estimation. The parameter estimation results demonstrate that the physics-based inverse method applied by this thesis can successfully estimate hydraulic conductivities.

Fig 4.1: Design of MODEL 1 (cross symbol: heads sampling locations; star symbol: flux sampling locations)
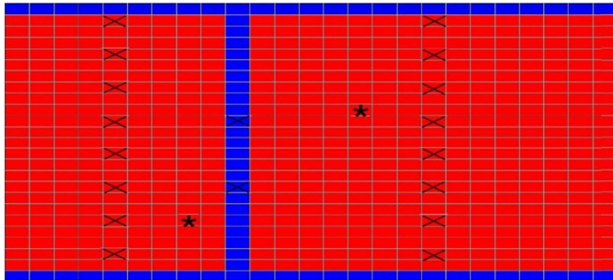

Fig 4.2: Design of MODEL 2 (cross symbol: heads sampling locations; star symbol: flux sampling locations)
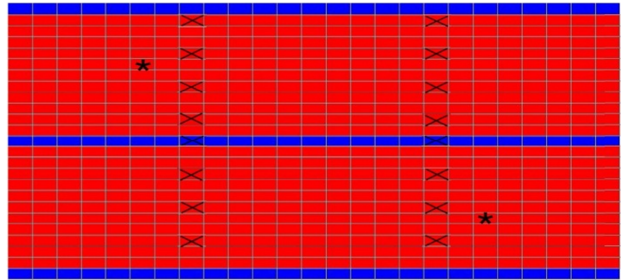

Fig 4.3: Design of MODEL 3 (cross symbol: heads sampling locations; star symbol: flux sampling locations)
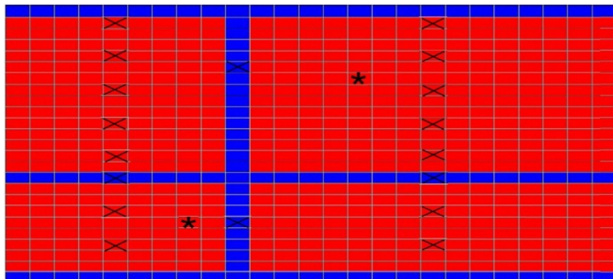

Fig 4.4: Design of MODEL 4 (data sampling strategy is the same as MODEL 2 shown in Fig 4.2)
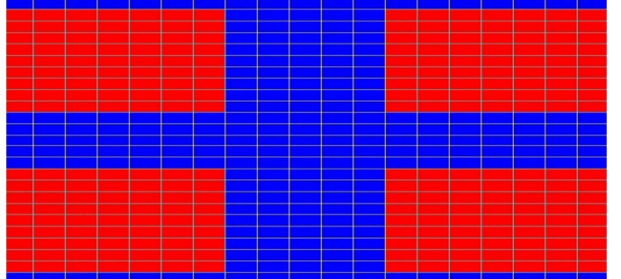
Table 4.1: Error Summary of the Inversions when $Kf / Km = 10$

MODEL	1	2	3	4
Error	0	4.57%	5.29%	0.70%

Instead of single horizontal or vertical fractures in previous models, MODEL 5 (Fig 4.5) is designed to have a more realistic fracture distribution which contains a set of diagonal fractures. For this model, multiple parameter estimation experiments are performed under the same observation data density of 57 hydraulic heads and 10 Darcy flux vectors (In this sampling strategy, the idea is that adequate observation data is available for parameter estimation, so the data locations are not specified in Fig 4.5). Parameter estimation is performed under different K_f/K_m values (ranging from 10^1 to 10^6). The inversion results of MODEL 5 are summarized in Table 4.2. When fracture conductivity is 10 times greater than matrix conductivity, hydraulic conductivity is underestimated by 4.44%; when fracture conductivity is 100 times greater than matrix conductivity, hydraulic conductivity is overestimated by 2.49%; when fracture conductivity is 1000 times greater than matrix conductivity, hydraulic conductivity is overestimated by 4.92%; and when fracture conductivity is 10^4 to 10^6 times of matrix conductivity, hydraulic conductivity is overestimated by approximately 5.24% to 5.27%. With the 6 parameter estimation experiments, the accuracy of hydraulic conductivity estimation by the physics-based inverse method is found to be not sensitive to the variability between fracture conductivity and matrix conductivity.
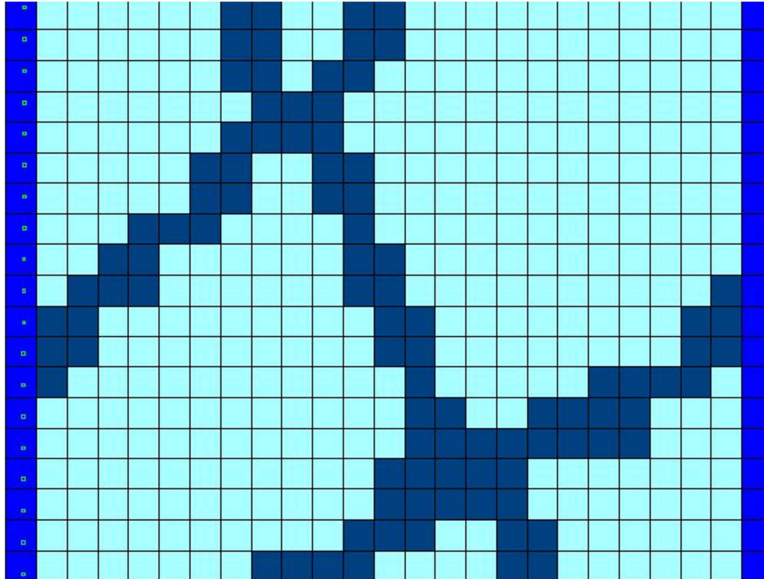
18

Fig 4.5: Design of MODEL 5

Table 4.2: Error Summary of the Inversions of MODEL 5

Ratio	10^1	10^2	10^3	10^4	10^5	10^6
Error	-4.44%	2.49%	4.92%	5.24%	5.27%	5.27%

2. Data Quality

The previous parameter estimations are performed utilizing true observation data without imposing measurement errors. It's possible to exclude measurement errors from previous inversions because synthetic true forward models are defined and the observation data are obtained by running the true forward models. However, it's inevitable to include measurement errors to observation data in real field work. Some of the errors may be caused by accuracy of the measurement equipment, and some may be caused by operators or other reasons.

As a result, we cannot assume that the observation data utilized by inversion are 100% accurate. Instead, errors should be applied to observation data manually, and the robustness of this physics-based inverse method when the observation data contain error must be tested. In this way, the practicability of this method can be demonstrated. In order to find out how measurement errors will influence the estimated parameter values, inversions are again performed for MODEL 4 (Fig 4.4) with the observation data containing either 5% or 10% measurement error.

Two different strategies are adopted to impose errors in order to get observation data with 5% measurement error. The first strategy imposes a random error between -5% and 5% to each observation data while the errors sum up to 0; the second strategy imposes errors of either -5% or 5% to each observation data. For both strategies, the errors are unbiased (the errors add up to 0). The same error imposing strategies are applied to get observation data with 10% measurement errors.

The true parameter values of MODEL 4 are summarized in Table 4.3, and the parameter estimation results obtained by inversions utilizing observation data with errors are summarized in Table 4.4. Note that when observation data available for inversion contain measurement errors, the parameter estimation results by the physics-based inverse method will degrade to a certain extent. The parameters estimated by data with 10% error are less accurate compared to the parameters estimated by data with 5% error, no matter which error imposing strategy is applied. As a result, the parameter estimation error will increase if the measurement error is greater. On the other hand, for a fixed amount of measurement error (e.g. 5%), estimated parameters are more accurate when the 1st error imposing strategy is applied (errors are between -5% and 5%),

and less accurate parameters will be obtained if the 2nd error imposing strategy (errors are either -5% or 5%) is applied. When measurement error is 5%, the parameter estimation errors are 16% (errors are between -5% and 5%) and 34% (errors are either -5% or 5%); when measurement error is 10%, the parameter estimation errors are 39% (errors are between -5% and 5%) and 65% (errors are either -5% or 5%). Even though the parameter estimation accuracy degrades when observation data contain error, the estimated parameter values are still reasonable and within the same order of true parameter values. The parameter estimation results in this section indicate that the physics-based inverse method does not collapse and still achieves acceptable parameter estimation results when observation data contain as high as 10% measurement error.

Table 4.3: True Parameter Values of MODEL 4

	Model 4	
Unit, ft/day	K_{matrix}	$K_{fracture}$
True	1	10

.

Table 4.4: Inversion Results when Observation Data Contain Error

Error	5%		10%	
Strategy	between -5% and 5%	either -5% or 5%	between -10% and 10%	either -10% or 10%
K_{matrix}	0.84	0.66	0.61	0.35
$K_{fracture}$	8.4	6.6	6.1	3.5

3. Streamlines & Recovered Boundary Conditions

The knowledge of streamlines is very useful in fluid dynamics. For MODEL 6 to MODEL 9, the physics-based inversion is performed to recover streamlines and boundary conditions under the same observation data density.

For MODEL 6 to MODEL 9 (Fig 4.6a to Fig 4.9a), the top boundaries are defined as constant head boundaries with hydraulic heads decreasing linearly from 600 ft on the left to 505 ft on the right. The left, bottom, and right boundaries are no flow boundaries.

MODEL 6 and MODEL 7 have flow barriers with lower hydraulic conductivities compared to the formation matrix, while MODEL 8 and MODEL 9 have high K faults with higher hydraulic conductivities compared to the matrix. The flow barriers in MODEL 6 and MODEL 7 have different orientations. The high K fault in MODEL 8 has the same orientation as the flow barrier in MODEL 6, and the high K fault in MODEL 9 has the same orientation as the flow barrier in MODEL 7. For all 4 models, the hydraulic conductivity of the formation matrix is defined as 1 ft/day. Hydraulic conductivity of flow barriers in MODEL 6 and MODEL 7 is 0.1 ft/day, and hydraulic conductivity of the high K faults in MODEL 8 and MODEL 9 is 10 ft/day.

Inversions are performed to obtain the estimated hydraulic conductivities. The hydraulic heads of each grid cell are calculated by the inversion process. As a result, the heads along the model boundary can be picked out as the inverted boundary conditions. This is how the physics-based inverse method recovers boundary conditions. The inverted streamlines of MODEL 6 to MODEL 9 are also achieved utilizing the inverted boundary conditions and inverted hydraulic conductivities (Fig 4.6b to Fig 4.9b). The true streamlines of MODEL 6 to MODEL 9 are generated with true boundary conditions (constant head boundaries and no flow boundaries) and

true hydraulic conductivity values (Fig 4.6a to Fig 4.9a). Both the true streamlines and the recovered streamlines are obtained by GW vista. The true boundary conditions and the inverted boundary conditions of MODEL 6 to MODEL 9 are plotted and compared in Fig 4.6c to Fig 4.9c. The parameter estimation results of MODEL 6 to MODEL 9 are summarized in Table 4.5a and Table 4.5b.

For Figure 4.6c to Figure 4.9c (boundary condition comparison), the bottom left grid cell of each model domain is defined as cell number 1 (on the horizontal axis of Fig 4.6c to Fig 4.9c). The cell number increases when moving up to the top left cell along the left boundary, moving right to the top right cell along the top boundary, moving down to the bottom right cell along the right boundary, and finally moving left to the second left grid cell along the bottom boundary. Red dashed lines represent true boundary conditions defined in forward models, and blue dashed lines are inverted boundary conditions.

By comparing the inverted boundary conditions to true boundary conditions, we note that MODEL 6 and MODEL 9 have very good fits without obvious discrepancies; MODEL 7 has some misfits on the bottom boundary; and MODEL 8 has some misfits on the left and bottom boundaries. Overall, the inverted boundary conditions fit the true boundary conditions very well, especially for MODEL 9 where an almost perfect fit to true boundary conditions is achieved. With these 4 comparisons, the physics-based inverse method is demonstrated to be capable of recovering boundary conditions while estimating parameters by the inversion process.

MODEL 6 has the biggest parameter estimation error of 17%; MODEL 9 has the smallest parameter estimation error of 5%. Due to the bigger hydraulic conductivity estimation error in MODEL 6, there are some misfits between the inverted streamlines (Fig 4.6b) and true

streamlines (Fig 4.6a) of MODEL 6. Overall, the inverted streamlines can represent true streamlines very well for all 4 models. Thus the physics-based inverse method is capable of recovering streamlines.

Table 4.5a: Parameter Estimation Results of MODEL 6 & 7

ft/day	Model 6		Model 7	
	K_{matrix}	$K_{barrier}$	K_{matrix}	$K_{barrier}$
True	1	0.1	1	0.1
Inverted	0.83	0.083	0.86	0.086

Table 4.5b: Parameter Estimation Results of MODEL 8 & 9

ft/day	Model 8		Model 9	
	K_{matrix}	K_{fault}	K_{matrix}	K_{fault}
True	1	10	1	10
Inverted	1.08	10.8	1.05	10.5

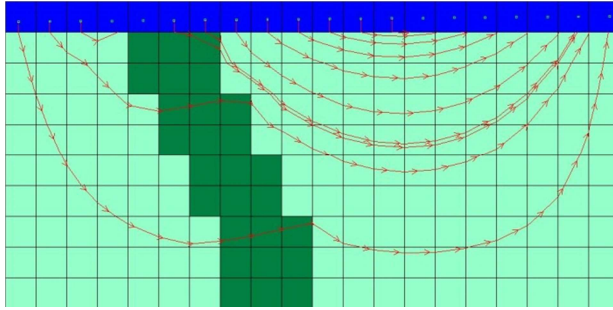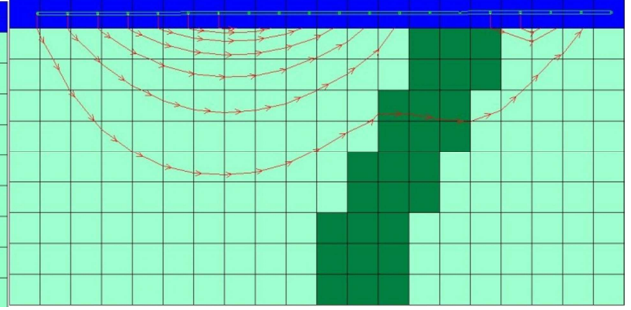Fig 4.6a: True Streamline of MODEL 6   Fig 4.7a: True Streamline of MODEL 7

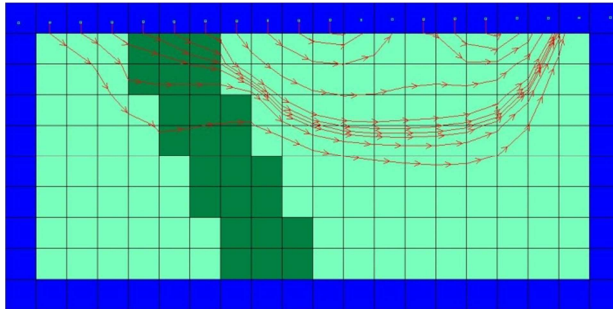Fig 4.6b: Inverted Streamline of MODEL 6   Fig 4.7b: Inverted Streamline of MODEL 7
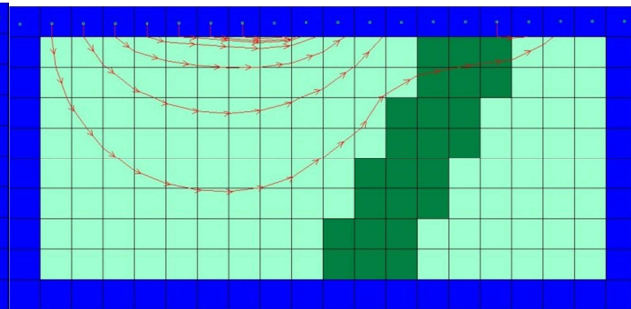

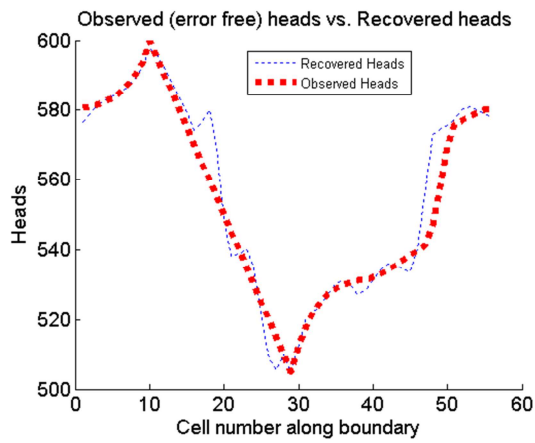Fig 4.6c: True BC vs. Inverted BC of MODEL 6   Fig 4.7c: True BC vs. Inverted BC of MODEL 7
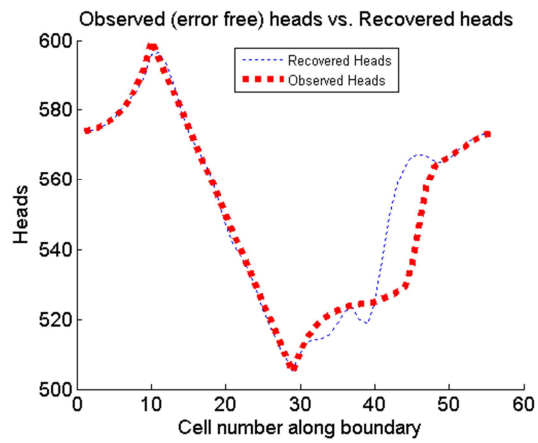
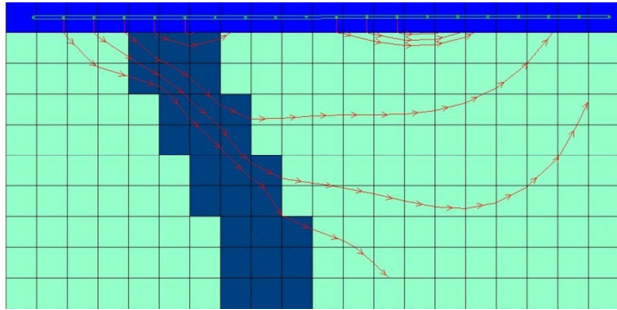Fig 4.8a: True Streamline of MODEL 8   Fig 4.9a: True Streamline of MODEL 9
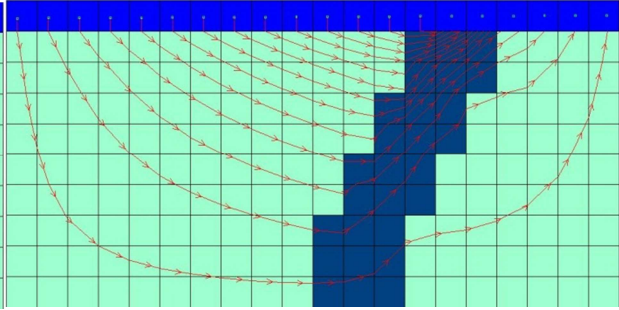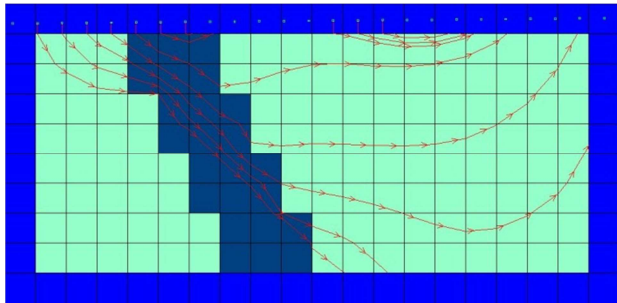

Fig 4.8b: Inverted Streamline of MODEL 8   Fig 4.9b: Inverted Streamline of MODEL 9
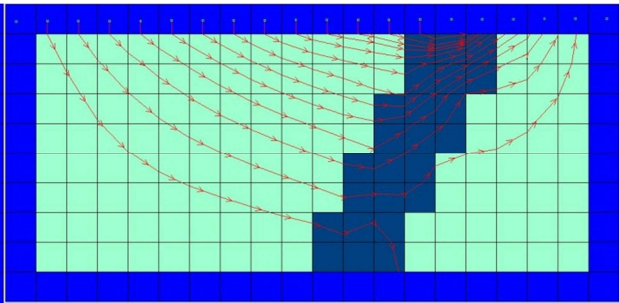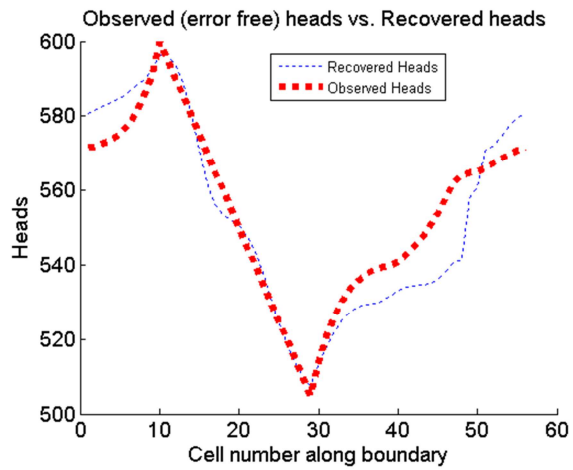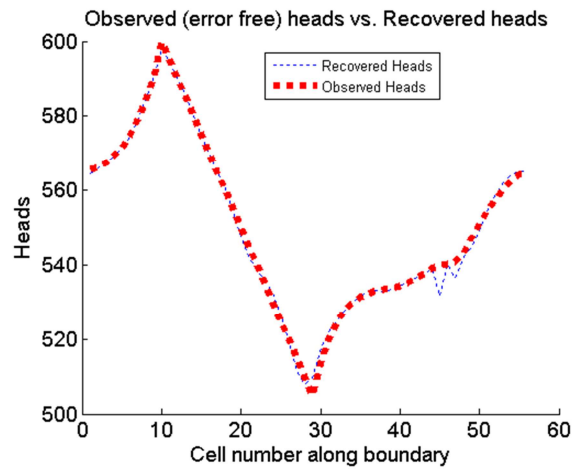

Fig 4.8c: True BC vs. Inverted BC of MODEL 8   Fig 4.9c: True BC vs. Inverted BC of MODEL 9

4. Parameter Estimation by PEST with Boundary Conditions Containing Error

One of the most significant advantages of this inverse method is that it does not require boundary conditions as an input; instead, this method can recover boundary conditions. In contrast, most of the existing parameter estimation methods involve multiple forward simulations to optimize an objective function. The first forward simulation requires the assumption of boundary conditions, which are usually (if not always) unknown. As a result, the presumed boundary conditions will certainly contain errors, or sometimes the assumed boundary conditions may even be wrong and leading to wrong parameter estimation results.

PEST is one of the most widely used source codes (software) in groundwater studies to perform parameter estimation and uncertainty analysis. The parameter estimation process by PEST requires known boundary conditions as most of the existing techniques do. Numerical experiments are performed in this thesis utilizing PEST to find out how the errors contained in the presumed boundary conditions affect the parameter estimation results. Eight parameter estimation experiments are performed for MODEL 8 under 4 different set of boundary conditions. The inversions are started with 2 different sets of initial guesses for each boundary condition. One set of the initial guesses is very close to the true parameter values, and the other set of the initial guesses is far away from true parameter values.

The true matrix conductivity of MODEL 8 is 1 ft/day, and the true fracture conductivity is 10 ft/day, which can be found in Table 4.5b. The 1st boundary condition tested is the true boundary condition which is represented by the blue lines in Fig 4.10. The 2nd boundary condition contains 5% or -5% error applied to the hydraulic heads on each grid cell along the boundary, which is represented by the red line in Fig 4.10a. The 3rd boundary condition contains an overall 5% error applied along the entire boundary, and the error is unbiased and adds up to 0. It is represented by

the green line in Fig 4.10b. The 4th boundary condition contains an overall 10% error applied to hydraulic heads along the boundary. The error for the 4th boundary condition is also unbiased, and the boundary condition is represented by the red line in Fig 4.10c.
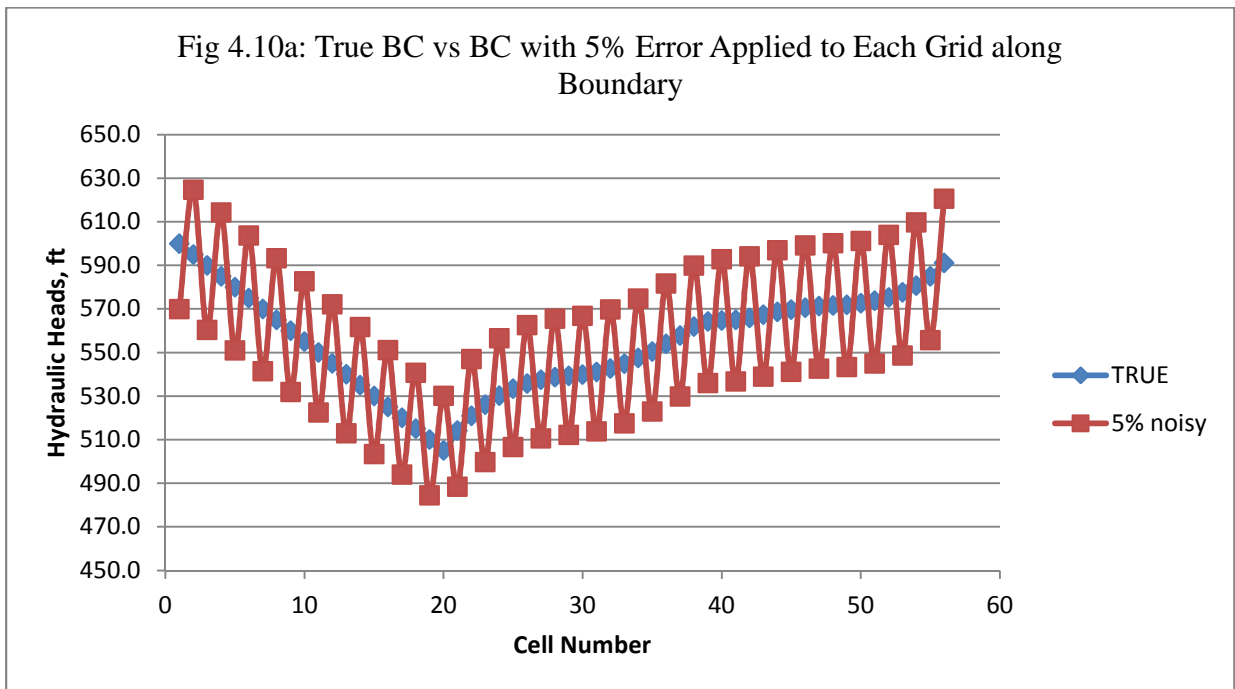
The inversion results of the eight numerical experiments performed by PEST are summarized in Table 4.6a and Table 4.6b. The results demonstrate that PEST can converge to the true parameter values when it is given the true boundary condition, no matter if the initial guess of parameter values is close to or far away from the true values. But when PEST is given a boundary condition that contains error, it will only converge to the true parameter values when the initial guess is close enough to the true values. If the initial guess is very different from true parameter values, PEST will not converge to the true values.

If the boundary condition that is given to PEST contains error on every grid cell along the boundary as in the 2nd case, PEST will converge to values with the same order of true parameter values when the initial guess is close enough to the true values. However, when the initial guess is far from the true values, the parameter values estimated by PEST are 2 orders smaller compared to the true values. This example shows that under the 2nd kind of boundary condition, PEST will only achieve an acceptable (but not very good) parameter estimation result when the initial guess is close enough to the true parameter values.

On the other hand, when the boundary condition given to PEST is smooth as in the 3rd case and in the 4th case, PEST will converge to the true parameter values if the initial guess is close to the true values, no matter if the amount of error contained in the boundary condition is 5% or 10%. When the initial guess is far away from true parameter values, the estimated values by PEST are still within the same order of the true values. But the percent of error is large. The parameter

estimation error is about 40% when the boundary condition contains 5% error. The errors

increase to 120% (matrix conductivity) and 218% (fracture conductivity) when then boundary

condition contains 10% error.

The results demonstrate that PEST is only reliable for estimating parameters when true boundary

conditions are known. In contrast, as the physics-based inverse method does not require known

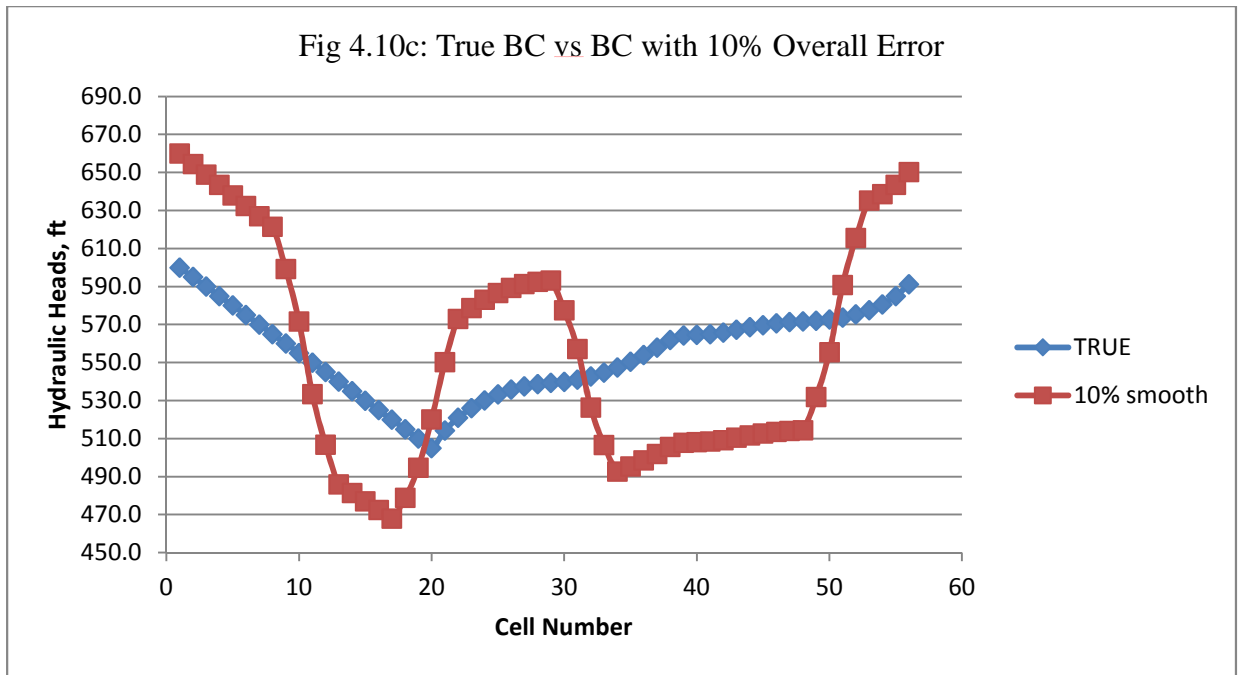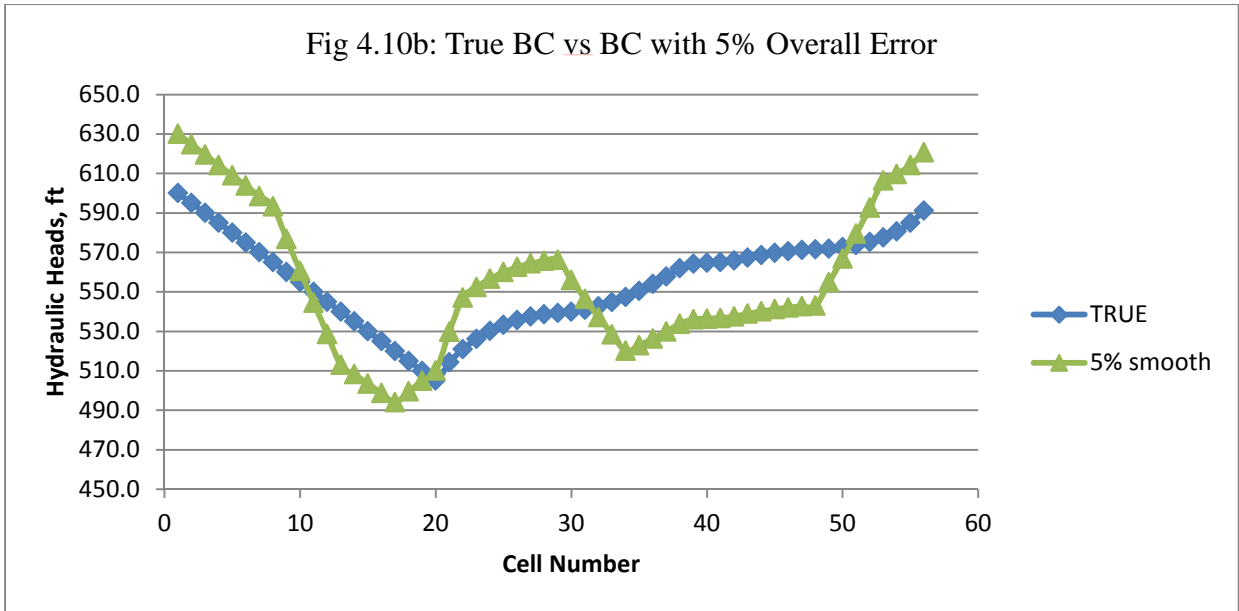boundary conditions in advance, it is more reliable for parameter estimations.

Fig 4.10a: True BC vs BC with 5% Error Applied to Each Grid along Boundary

Fig 4.10b: True BC vs BC with 5% Overall Error

Fig 4.10c: True BC vs BC with 10% Overall Error

Table 4.6a: Inversion Results with True BC by PEST

Initial value (ft/day)		True BC	
K_{matrix}	K_{frac}	K_m	K_f
1	10	1	10
0.01	1000	1.04	10.4

Table 4.6b: Inversion Results with Different BCs by PEST

Initial value (ft/day)		5% noisy		5% smooth		10% smooth	
K_{matrix}	K_{frac}	K_m	K_f	K_m	K_f	K_m	K_f
1	10	1.9	5.3	1	10	1	10
0.01	1000	0.06	0.13	0.56	6.07	2.2	31.8

5. Effective Conductivity Estimation

Hydraulic conductivity heterogeneity is one of the most significant factors that influence groundwater flow. Studies have proved that spatial variation of hydraulic conductivity (similar to permeability in petroleum engineering) exists in all natural sedimentary deposits. The importance of conductivity heterogeneity depends on the scale of problems. For example, conductivity heterogeneity is less crucial for estimating bulk flow characteristics. In typical regional to basin-scale groundwater studies, conductivity heterogeneity is usually not incorporated into flow

models because the cost of conducting detailed sampling over large spatial scales is very high. However, reasonable results can still be obtained without detailed heterogeneity information. Also it's very difficult to incorporate detailed conductivity heterogeneity into models due to current computational limits. Sedimentary deposits are commonly represented by a series of internally homogeneous hydrogeological units (Zhang, Gable, & Person, 2006). Lateral and vertical conductivity heterogeneity within each unit is ignored. The equivalent conductivity represents a fictitious homogeneous deposit for a given head gradient. The estimation of the equivalent conductivity can be performed by numerous methods. The equivalent conductivity depends on the boundary condition, thus it is not unique when the boundary condition changes.

All the previous parameter estimations are performed for deterministic models, where the spatial distribution of hydraulic conductivity is known. This is the ideal case as the forward models are defined synthetically, and the exact distribution of hydraulic conductivity is known. However, when the spatial distribution of hydraulic conductivity is unknown, the effective K (upscaled K) on both the x direction and the z direction can be estimated. As the true forward model is known, the true boundary conditions are also known and unique. As a result, the analytically calculated effective hydraulic conductivity is also unique. This analytical effective conductivity value is used as the criteria to test the accuracy of the effective conductivity estimated by inversion.

In MODEL 8 and MODEL 5, when the fracture hydraulic conductivity is 10 times greater than matrix conductivity, the effective K on x and z directions are estimated both numerically and by inversion. The estimated K by inversion is obtained by the physics-based inverse method. Before estimating effective conductivity, the forward models are redefined. First, the left and right boundaries are defined as constant head boundaries; the top and bottom boundaries are no flow

32

boundaries (both MODEL 8 and MODEL 5). In this case, flow only occurs on x direction. Then this new defined forward model is run to obtain observation data of hydraulic heads and horizontal Darcy fluxes. Then the entire study area is assumed to be homogeneous and all the grid cells have the same hydraulic conductivity value. Under this assumption, the physics-based inversion is again performed and the calculated hydraulic conductivity value is the effective conductivity on the x direction. Second, the left and right boundaries of the forward models are defined as no flow boundaries; the top and bottom boundaries are constant head boundaries. In this case, only vertical flow occurs. Then the first step is repeated to obtain the effective conductivity on the z direction.

The results of effective K estimation for MODEL 8 are summarized in Table 4.7. The effective K estimation on the x direction is less accurate than the effective K estimation on the z direction. This is because MODEL 8 exhibits more heterogeneity on the x direction. The results of effective K estimation for MODEL 5 are summarized in Table 4.8. This model exhibits equal heterogeneity on the x and z directions. As a result, the effective K estimations are almost equally accurate on both directions. On the other hand, the estimated effective K of MODEL 5 is more accurate than the estimated effective K of MODEL 8. The reason is due to the more equally distributed heterogeneity in MODEL 5 compared to that of MODEL 8. In other words, the formation represented by MODEL 5 is closer to a homogeneous medium than the formation represented by MODEL 8. So the effective K of the more homogeneous medium can be estimated more accurately by inversion.

The results in Table 4.7 and Table 4.8 indicate that the physics-based inverse method can achieve good estimations of effective hydraulic conductivities.

Table 4.7: Inversion Results of Upscaled K of MODEL 8

	Model 8	
Unit, ft/day	K_{xx}	K_{zz}
Numerically upscaled K	1.27	2.27
Inversed upscaled K	0.93	2.36

Table 4.8: Inversion Results of Upscaled K of MODEL 5

	Model 5	
Unit, ft/day	K_{xx}	K_{zz}
Numerically upscaled K	1.77	1.88
Inversion upscaled K	1.80	1.88

6. Comparison of True Flow Fields and Inverted Flow Fields

The physics-based inversion can also be applied to recover flow fields, as well as to estimate hydraulic conductivities. The inverted flow fields are obtained by running forward models with inverted hydraulic conductivities and inverted boundary conditions. Then the inverted flow fields are compared to the true flow fields to determine how well they fit each other.

In MODEL 6 ($K_{barrier}$ = 0.1 ft/day; K_{matrix} = 1 ft/day), true streamlines (Fig 4.6a) and true velocity vector fields (Fig 4.11a) are compared to inverted streamlines (Fig 4.6b) and inverted

velocity vector fields (Fig 4.11b). The comparison shows that the inverted streamlines fit the true streamlines very well. The main discrepancy between true and inverted velocity vector fields occurs within the flow barrier area. The true velocity in the flow barrier is much lower than the velocity in the matrix. However, there is no significant difference between the inverted velocity in the flow barrier and the velocity in the matrix. Also the contour of the true head field (Fig 4.12a), contour of true horizontal fluxes (Fig 4.12b), and contour of true vertical fluxes (Fig. 12c) are plotted for comparison with the contour of the inverted head field (Fig 4.13a), contour of inverted horizontal fluxes (Fig 4.13b), and contour of inverted vertical fluxes (Fig 4.13c). The contour of the inverted head field represents the contour of the true head field very well with the major difference occurring around the flow barrier region. The contours of true fluxes (both horizontal and vertical) are very smooth. However, the contours of inverted fluxes are noisier. But overall the inverted contours recover the main characters of the true contours, with all the major differences located within the flow barrier region. This comparison shows that when the ratio between two different flow units' hydraulic conductivities is 10, the physics-based inverse method can recover the major flow characters well.

Then in order to explore how the inverted flow fields recover the true flow fields when the ratio of hydraulic conductivities is higher, the same analysis is performed for MODEL 7. The parameter values are adjusted to $K_{barrier} = 0.001$ ft/day and $K_m = 1$ ft/day. True streamlines (Fig 4.14a) and true velocity vector fields (Fig 4.15a) are compared to inverted streamlines (Fig 4.14b) and inverted velocity vector fields (Fig 4.15b). The inverted streamlines fit the true streamlines on the large scale, with some local misfits. The main discrepancies between true and inverted velocity vectors locate around the flow barrier region and along part of the model boundary. Also the contour of the true hydraulic head field (Fig 4.16a), contour of true horizontal fluxes (Fig

4.16b), and contour of true vertical fluxes (Fig 4.16c) are plotted to compare with the contour of

the inverted hydraulic head field (Fig 4.17a), contour of inverted horizontal fluxes (Fig 4.17b),

and contour of inverted vertical fluxes (Fig 4.17c). The contour of inverted heads is quite

different from the contour of true heads around the flow barrier region. Other than that, the

inverted head contour fit the true head contour well. On the other hand, the contours of inverted

horizontal and vertical fluxes are noisy and have a lot of discrepancies with the true contours of

fluxes. These discrepancies occur in different regions of the model domain and are not limited to

the flow barrier. This comparison shows that when the ratio between matrix conductivity and

flow barrier conductivity increases to 1000, the physics-based inverse method can recover some

of the flow characters. Even though there are some misfits, the inverted velocities fall in the

same range with true velocities. The horizontal flow velocities (both true and inverted) are

between -0.4 ft/day and 1.2 ft/day, and the vertical flow velocities (both true and inverted) are

approximately between -0.5 ft/day and 0.5 ft/day.

In MODEL 5 (K_f/K_m equals 10), true streamlines (Fig 4.18a) are compared to inverted

streamlines (Fig 4.18b). In this comparison, the inverted streamlines achieve an almost perfect fit

to true streamlines. This is probably caused by the more linear true streamlines in MODEL 5

compared to the highly non-linear streamlines in MODEL 6 and MODEL 7. There is no obvious

discrepancy between the true and inversed streamlines. Also the contour of the true hydraulic

head field (Fig 4.19a), contour of true horizontal fluxes (Fig 4.19b), and contour of true vertical

fluxes (Fig 4.19c) are plotted to compare with the contour of the inverted hydraulic head field

(Fig 4.20a), contour of inverted horizontal fluxes (Fig 4.20b), and contour of inverted vertical

fluxes (Fig 4.20c). For all three pairs of comparisons, the inverted contours recover the true

contours very well, both in the fracture region and the matrix. Although the recovered contours

are a little noisier compared to the true contours (especially the inverted contour of hydraulic heads), there is no obvious discrepancy. This analysis shows that the physics-based inverse method can recover the flow characteristics of fracture systems well, when the ratio between the fracture conductivity and the medium conductivity equals 10.

Furthermore, by comparing the contour analysis of MODEL 5, MODEL 6, and MODEL 7, it's obvious that the physics-based inverse method recovers the flow fields better when the true streamlines are more linear (as of MODEL 5).

Fig 4.11a: True Velocity Vector Field of MODEL 6
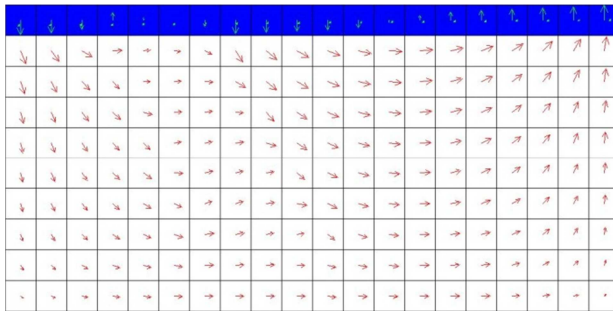
Fig 4.11b: Inverted Velocity Vector Field of MODEL 6
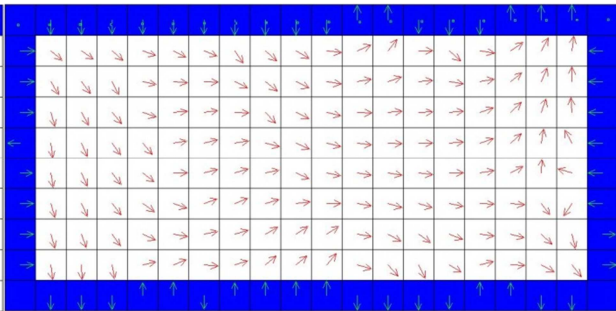
Fig 4.12a: Contour of True
Head Field of MODEL 6
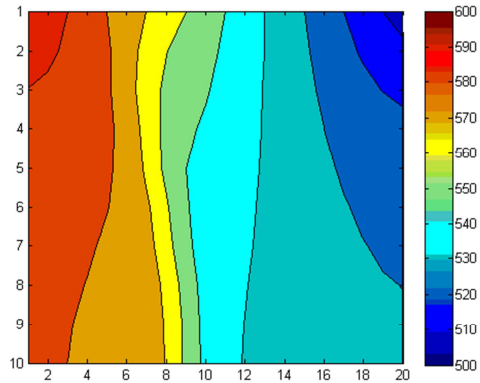
Fig 13a: Contour of Inverted
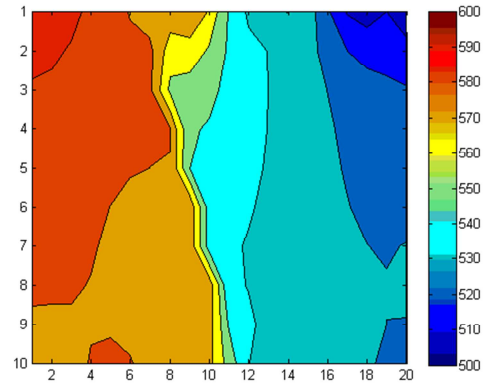Head Field of MODEL 6

Fig 4.12b: Contour of True
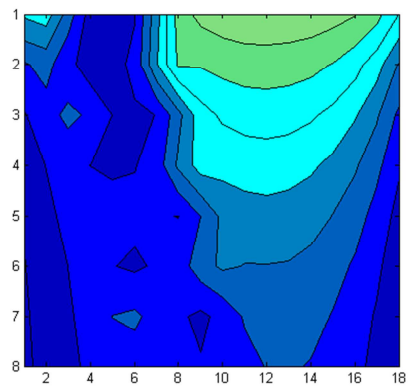Horizontal Flux of MODEL 6

Fig 4.13b: Contour of Inverted
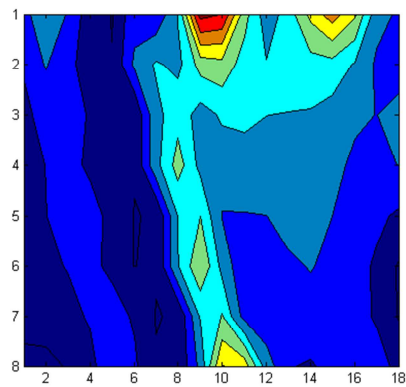Horizontal Flux of MODEL 6
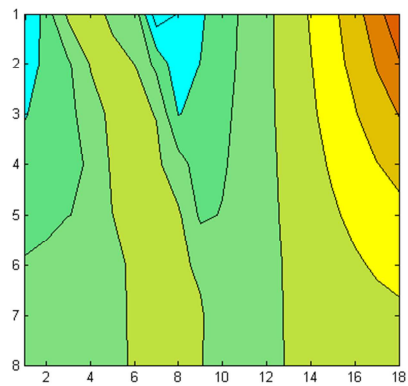

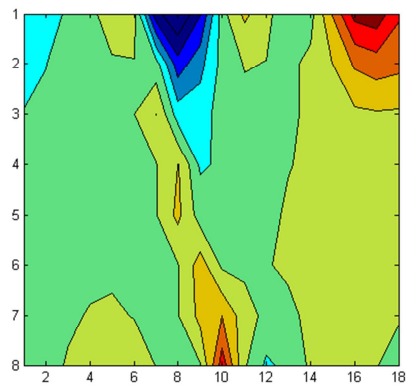Fig 4.12c: Contour of True
Vertical Flux of MODEL 6

Fig 4.13c: Contour of Inverted
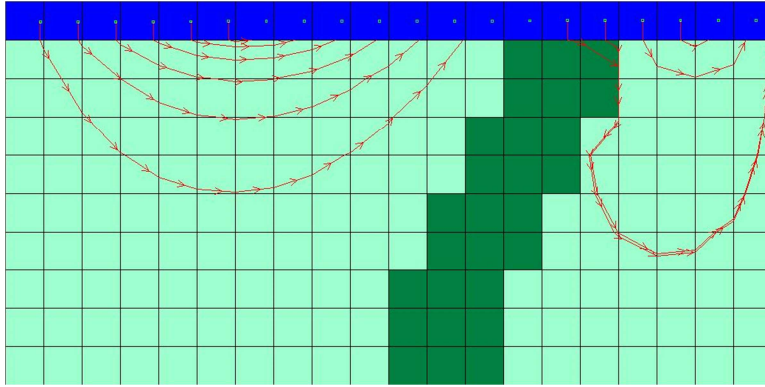Vertical Flux of MODEL 6

Fig 4.14a: True Streamline of MODEL 7 (Parameter Values Adjusted to $K_{barrier}$ = 0.001 ft/day; K_m = 1 ft/day)
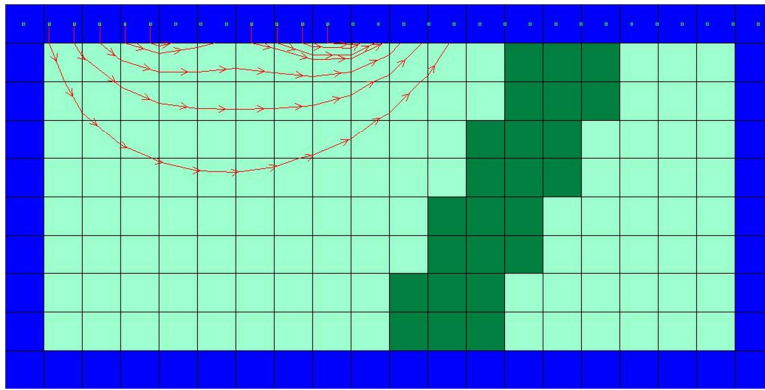

Fig 4.14b: Inverted Streamline of MODEL 7 (Parameter Values Adjusted to $K_{barrier}$ = 0.001 ft/day; K_m = 1 ft/day)
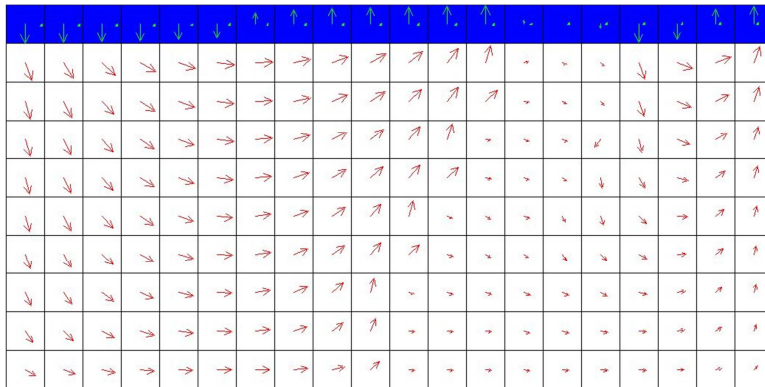

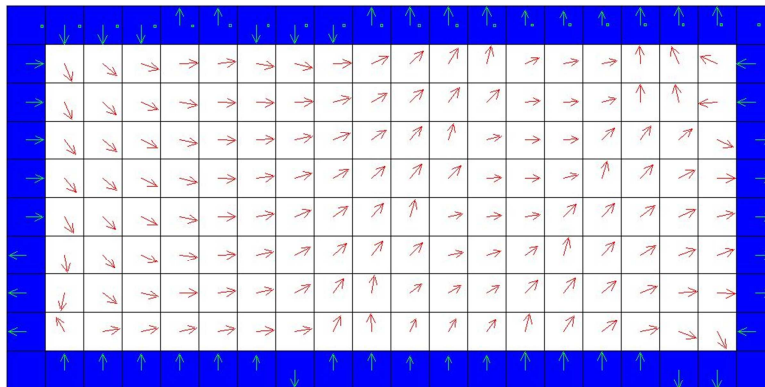Fig 4.15a: True Velocity Vector Field of MODEL 7 ($K_{barrier}$ = 0.001 ft/day; K_m = 1 ft/day)

Fig 4.15b: Inverted Velocity Vector Field of MODEL 7 ($K_{barrier}$ = 0.001 ft/day; K_m = 1 ft/day)

Fig 4.16a: Contour of True
Head Field of MODEL 7

Fig 4.17a: Contour of Inverted
Head Field of MODEL 7

Fig 4.16b: Contour of True
Horizontal Flux of MODEL 7

Fig 4.17b: Contour of Inverted
Horizontal Flux of MODEL 7

Fig 4.16c: Contour of True
Vertical Flux of MODEL 7

Fig 4.17c: Contour of Inverted
Vertical Flux of MODEL 7
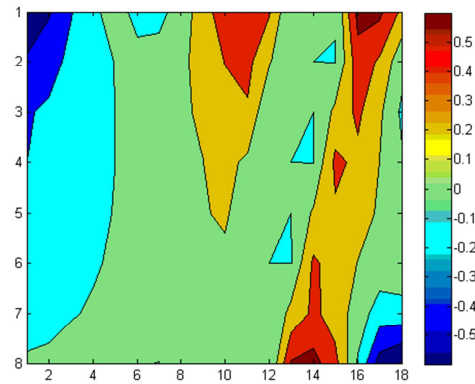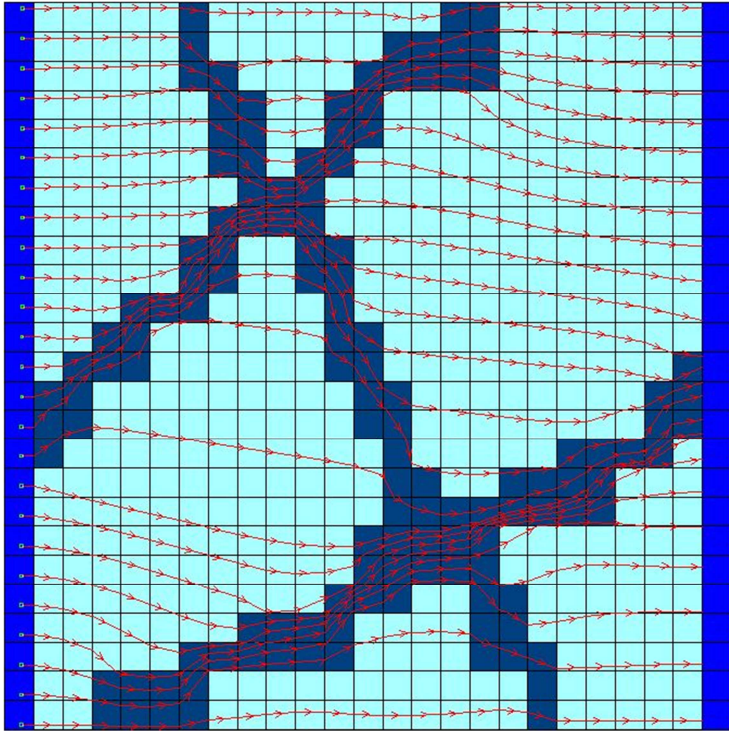
Fig 4.18a: True Streamline of MODEL 5 ($K_f/K_m = 10$)

Fig 4.18b: Inverted Streamline of MODEL 5 ($K_f/K_m = 10$)

Fig 4.19a: Contour of True
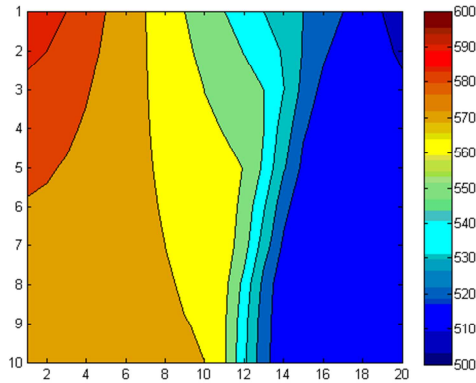Head Field of MODEL 5

Fig 4.20a: Contour of Inverted
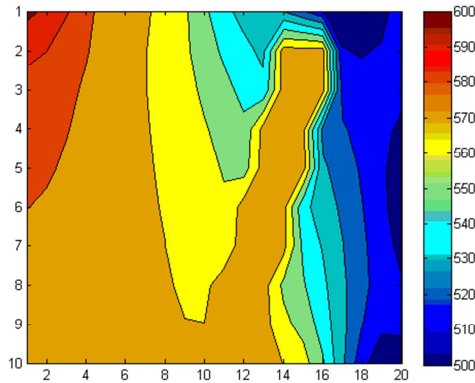Head Field of MODEL 5

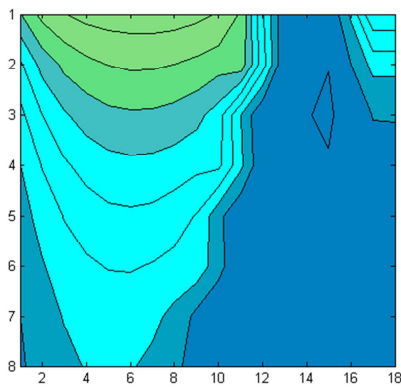Fig 4.19b: Contour of True
Horizontal Flux of MODEL 5

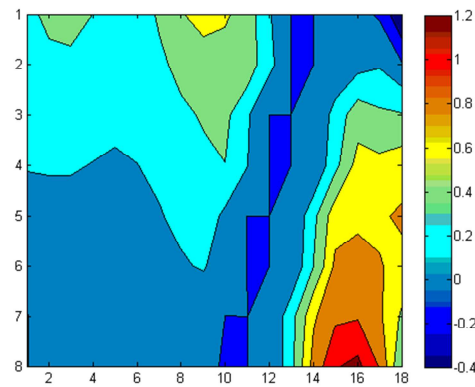Fig 4.20b: Contour of Inverted
Horizontal Flux of MODEL 5

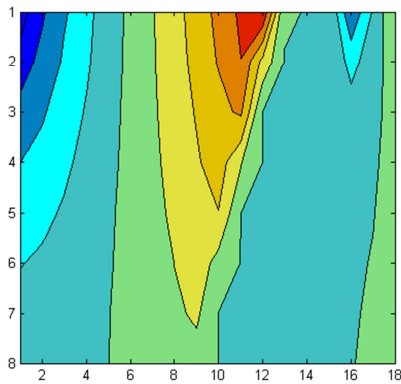Fig 4.19c: Contour of True
Vertical Flux of MODEL 5
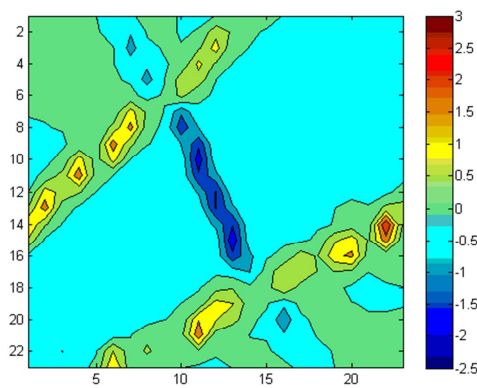
Fig 4.20c: Contour of Inverted
Vertical Flux of MODEL 5
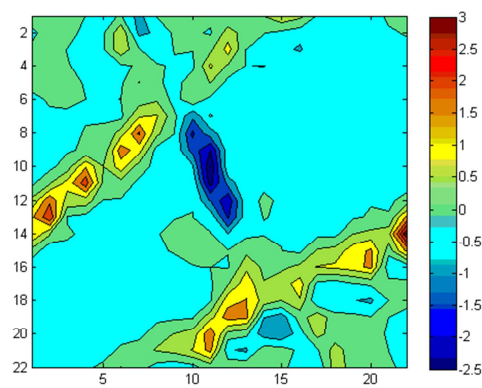
7. Uncertainty Analysis

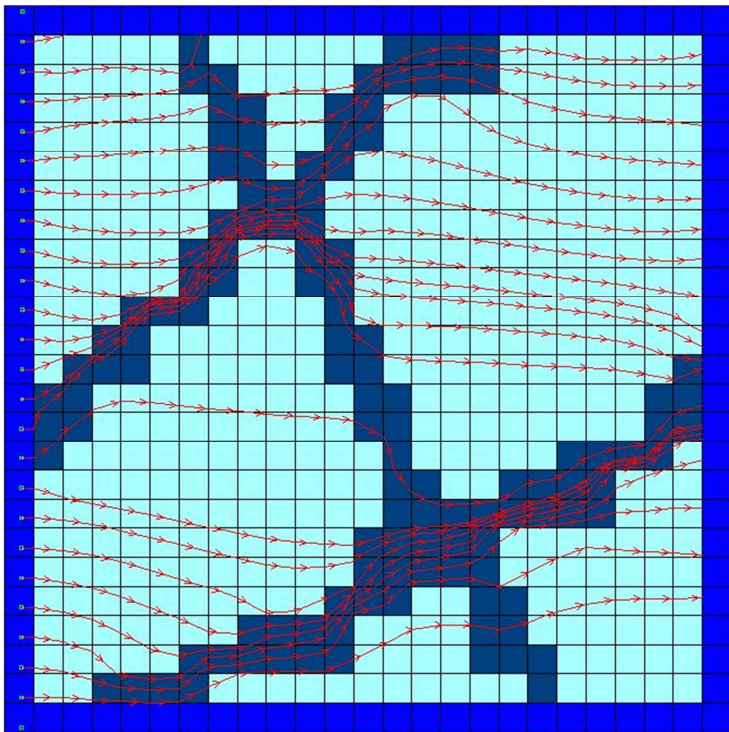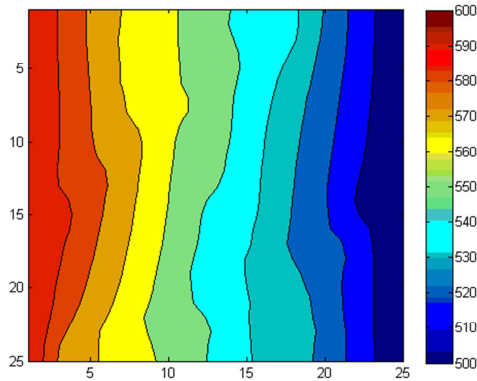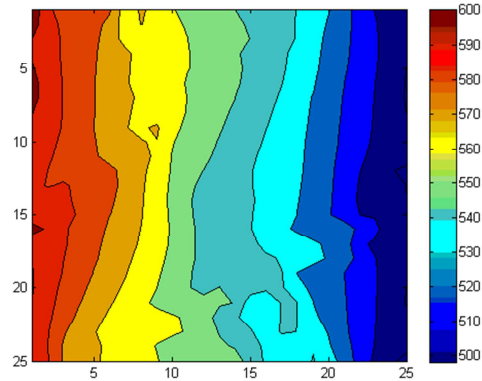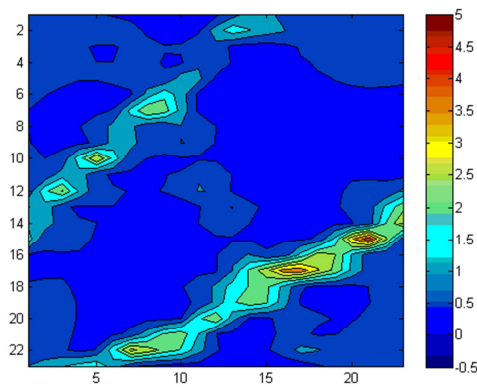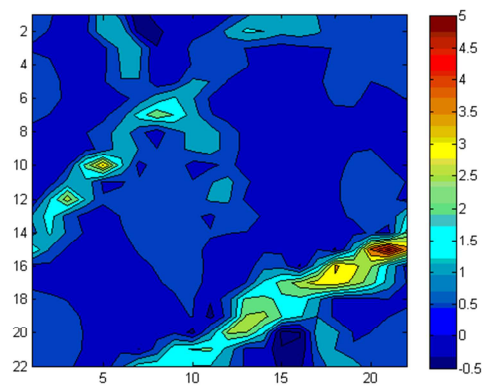Observation data (hydraulic heads and Darcy fluxes, in this thesis) sampling density is a major factor influencing parameter estimation accuracy. Usually, parameter estimation results will approach the true parameter values if more observation data is sampled. But sampling additional observation data will usually cost more. As a result, it is crucial to find out the optimum data density at which parameters can be estimated with satisfying accuracy and the cost of sampling data is also acceptable. So it will be useful to find out the trend of how parameter estimation accuracy changes with different observation data density.

A global inverse sensitivity analysis is performed by increasing the number of observation hydraulic heads from 10 to 250. A single Darcy flux vector is applied for inversion. Under each data density, 20 random simulations are performed. For each simulation, hydraulic heads are randomly sampled from the entire domain based on the data density. Hydraulic conductivity is then estimated utilizing the randomly sampled hydraulic heads and the fixed Darcy flux vector. The objective of this global uncertainty analysis is to find out the sensitivity of the parameter estimation accuracy to observation data density of this physics-based inverse method, and potentially find out the optimum observation data density.

The results of this global uncertainty analysis are summarized in Figure 4.21. The horizontal axis represents the number of observed hydraulic heads ranging from 10 to 250. The vertical axis on the left represents the inverted hydraulic conductivity values in the unit of ft/day. The inverted conductivity ranges from 0.25 ft/day to 0.285 ft/day. The true hydraulic conductivity equals 0.283 ft/day. The vertical axis on right represents the absolute values of parameter estimation errors ranging from 3% to 8%.

The stacked columns in this figure are the uncertainty analysis results. Under each observation data density, the lower boundary of the vertical error bar represents the smallest value of estimated hydraulic conductivity (corresponds to the vertical axis on the left), and the upper boundary of the vertical error bar represents the largest value of estimated hydraulic conductivity. The lower boundary of the red column represents the 25 percentile of the range of estimated hydraulic conductivity values at that data density; the boundary between the red column and the green column represents the 50 percentile of the range; and the upper boundary of the green column represents the 75 percentile of the range. At the data density of 10, the estimated hydraulic conductivity ranges from about 0.255 ft/day to more than 0.27 ft/day. Then as the data density increases, the range of estimated hydraulic conductivity values decreases. When the range decreases, the uncertainty of parameter estimation also decreases. When the hydraulic heads density reaches 250, the variation of estimated hydraulic conductivity values are very small, ranging between 0.27 ft/day and 0.275 ft/day. As a result, observation data density is critical for parameter estimation. The uncertainty of parameter estimation decreases when the observation data density increases.

Within each stacked column, the purple cross symbol represents the average value of estimated hydraulic conductivities under that data density. By connecting all cross symbols, the purple trend is achieved. It shows how the average parameter estimation values change with observation data density. When data density is 10, the average value of estimated hydraulic conductivities is about 0.26 ft/day. Then as the data density increases, the average value increases and approaches the true hydraulic conductivity value of 0.283 ft/day. When data density reaches 250, the average value is about 0.275 ft/day. This is very close to the true

parameter value. This trend shows that when observation data density increases, the expected value of the estimated parameter will approach the true parameter value.

The blue star symbol represents the absolute values of parameter estimation errors (calculated using the average parameter estimation value under each data density). The expected error is about 8% (reading from the vertical axis on the right) when only 10 hydraulic heads are sampled. Then as the data density increases, the expected error decreases significantly. When 250 hydraulic heads are utilized for inversion, the expected parameter estimation error is less than 3.5%. This trend shows that a lower parameter estimation error is guaranteed when more observation data is sampled.

Results of this global uncertainty analysis suggest that K_f estimation error is significantly influenced by the density of observed hydraulic heads (Fig 4.21). The inversion accuracy is very sensitive to observation data density. With increasing heads, K_f estimation accuracy increases and the estimation uncertainty decreases.

Fig 4.21: Uncertainty & Mean of Inverted Kf Values, and Inversion Errors
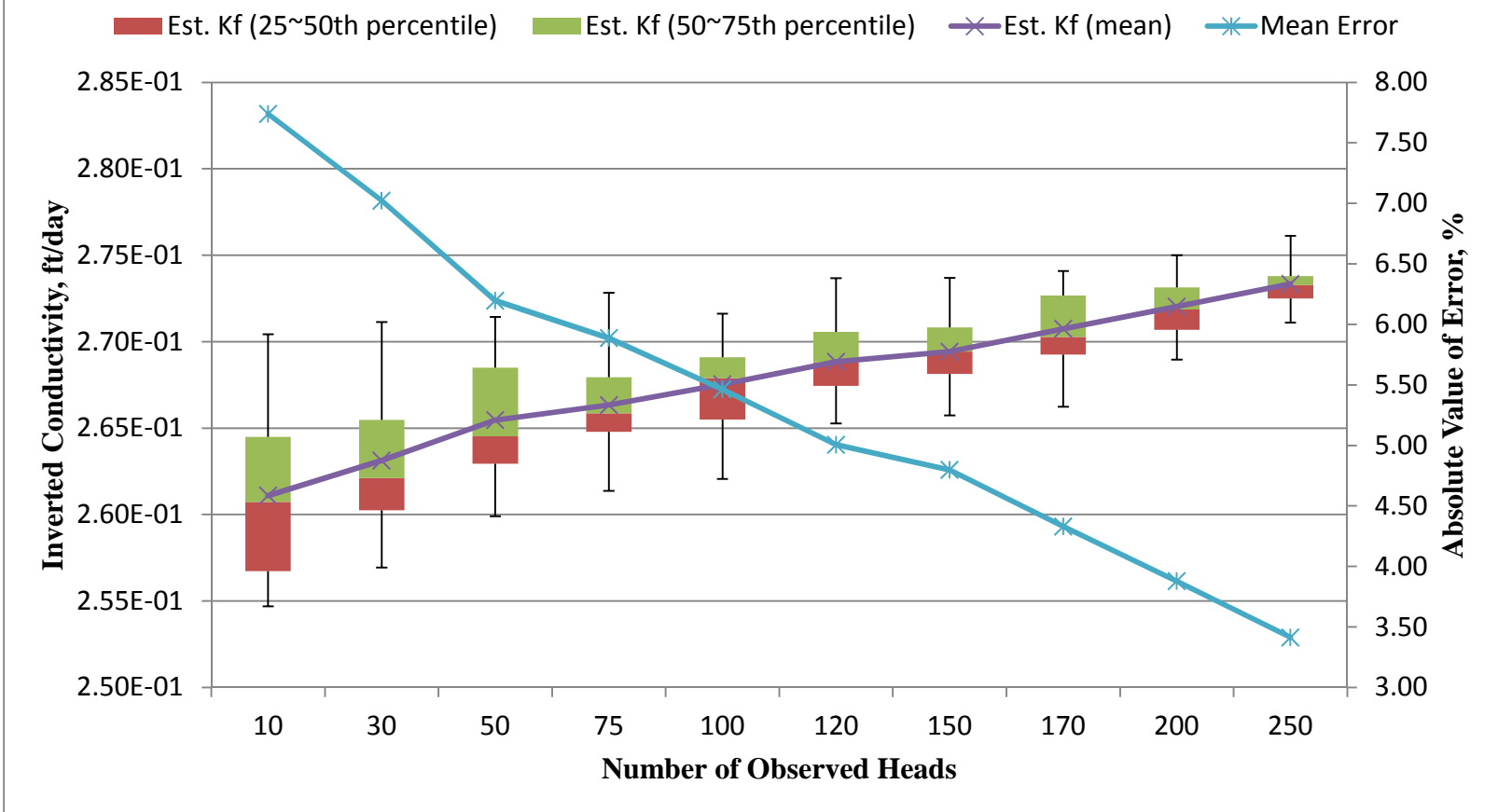
CHAPTER 5   CONCLUSION

The physics-based inverse method is tested for parameter and boundary condition estimations of steady state groundwater flow in fractured confined aquifers. The most significant advantage of this method lies in its computational efficiency as no repeated forward simulations are required. The noisy observation data (hydraulic heads containing measurement error) are directly incorporated into the solution matrix, which is solved in a one-step procedure to obtain both formation parameters and state variables.

This method is not sensitive to the ratio between fracture conductivity (K_f) and matrix conductivity (K_m) as hydraulic conductivities have been successfully estimated when this ratio ranges from 10 to 10^6. This method is also tested to be robust to data errors. Parameter estimations have achieved reasonable results when observation data (hydraulic heads) applied for inversion contain error up to 10%.

Boundary conditions have been recovered for problems that either include high conductivity fractures or low conductivity flow barriers. The recovered boundary conditions are compared to the true boundary conditions (boundary conditions defined in true forward models), and the misfits are found to be negligible. In addition, streamlines are also obtained using estimated hydraulic conductivities and recovered boundary conditions. The recovered streamlines capture the major characters of the true streamlines, though some misfits exist adjacent to the high conductivity (fractures) or low conductivity (flow barriers) zones.

Furthermore, the scientific importance of estimating boundary conditions is verified by PEST. Most of the traditional inverse methods require the presumption of boundary conditions. The assumed boundary conditions are essentially false observation data on each grid cell along the entire boundary. As a result, the inversion process is actually conducted with both true observation data and a significant amount of false observation data. Numerical simulations have been performed by PEST when the presumed boundary conditions contain either 5% or 10% error. The results suggest that the inversion will only converge to the true parameter values when the initial guesses are close enough to the true values. Other than that, the parameter estimation results are not satisfying.

Upscaled effective hydraulic conductivities that can represent flow in fractured aquifers are also estimated. Effective conductivities of two different models are estimated by inversion and then compared to theoretically calculated, effective conductivities. For both models, the estimated effective conductivities on both directions are very close to the theoretical values. As a result, this physics-based method is applicable to estimate effective hydraulic conductivities for fractured aquifers.

For three different models, the contour maps of inverted state variables (hydraulic head, horizontal Darcy flux, and vertical Darcy flux) are plotted and compared to the contours of corresponding true state variables. The inverted flux vectors are also compared to the true flux vectors. The contour maps of inverted values recover the most significant characteristics of the true contours with the major discrepancies located around the high conductivity fracture or low conductivity flow barrier zone. The main difference between the true and inverted flux vector

fields also lies in these areas. The inverted contours fit the true contours much better when the true streamlines in the forward model is more linear.

Finally, an uncertainty analysis is also conducted by increasing the number of observation hydraulic heads, while using a single Darcy flux vector for inversion. Results of this uncertainty analysis suggest that the parameter estimation error is significantly influenced by the density of observation data. With increasing heads (from 10 to 250) parameter estimation accuracy increases while its uncertainty decreases. As a result, the inversion accuracy is determined to be sensitive to data density.

APPENDIX

Reynolds Number (Re)

There are two basic types of fluid flow. When all molecules within the fluid move parallel to each other in the direction of flow, the flow is named laminar flow. If molecules in the fluid move in all directions but with a net movement in the flow direction, then the flow is named turbulent flow. There are also transition state flows between laminar flow and turbulent flow. In heterogeneous fluids, almost no mixing happens in laminar flows. On the other hand, heterogeneous fluids are thoroughly mixed when the flow state is turbulent flow.

For this thesis, Darcy's law is applied to calculate groundwater fluxes. There are two main issues associated with the usage of Darcy's law. The continuum assumption assumes that the microscopic pore-scale velocity variation can be represented by the volume-averaged macroscopic properties, such as flow rate, Darcy flux, and average linear velocity. In other words, microscopic pore-scale velocity variations are overlooked. The second issue is that Darcy's law applies only to laminar flows. It can be inappropriate to use Darcy's law if the groundwater velocity is large and the flow state is turbulent, which could be the case when groundwater flows through rocks with large pores.

In fluid mechanics, one of the most important parameters that characterize flows is the Reynolds number (Re). This parameter is named after Osborne Reynolds who documented the distinction between laminar and turbulent motion in the late 19th century. The Reynolds number is defined as the ratio of inertial forces to viscous forces and consequently quantifies the relative importance of these two types of forces for any given flow condition. The Reynolds number is a

dimensionless quantity that indicates the extent to which a flow is laminar or turbulent. The Reynolds number is defined by the following equation:

$$R_e = \frac{\rho q d}{\mu}$$

ρ: water density, M/L^3; constant, 1000 kg/m^3 at 4 °C;

q: magnitude of Darcy flux, L/T;

d: mean pore size, L;

μ: water viscosity, M/LT; constant, 0.001002 kg/(ms) at 20 °C;

Fluid flow is found to be laminar when the Reynolds number is low (<10) and turbulent when the Reynolds number is high (>2000). There is a transition from laminar flow to turbulent flow in the middle. With increased velocity, the Reynolds number will increase correspondingly, and the flow is more likely to be turbulent. But it is widely accepted that the flow state is laminar when the Reynolds number is no larger than 10.

In this thesis, as Darcy's law will be applied to calculate fluxes, the Reynolds number of each model is carefully investigated. As discussed before and the definition of the Reynolds number indicates, high values of Darcy fluxes may lead to a Reynolds number that is higher than 10 and Darcy's law is no longer applicable. The hydraulic head gradient of each model in this thesis is set to be not too large over the problem domain in order to guarantee that the Reynolds number of each model is smaller than 10, as thus Darcy's law stands.

REFERENCE

Abbas, F. (2000). Recovery mechanisms in fractured reservoirs and field performance. *Journal of Canadian Petroleum Technology*, *39*(11), 13–17.

Bayless, E. R., Mandell, W. A., & Ursic, J. R. (2011). Accuracy of flowmeters measuring horizontal groundwater flow in an unconsolidated aquifer simulator. *Ground Water Monitoring & Remediation*, *31*(2), 48–62. doi:10.1111/j1745-6592.2010.01324.x

Berkowitz, B. (2002). Characterizing flow and transport in fractured geological media: a review. *Advances in Water Resources*, *25*(8-12), 861–884. doi:10.1016/S0309-1708(02)00042-8

Bonnet, E., Bour, O., Odling, N. E., Davy, P., Main, I., Cowie, P., & Berkowitz, B. (2001). Scaling of fracture systems in geologic media. *Reviews of Geophysics*, *39*(3), 347–383.

Bourbiaux, B. (2010). Fractured reservoir simulation: a challenging and rewarding issue. *Oil & Gas Science and Technology – Revue de l'Institut Français Du Pétrole*, *65*(2), 227–238. doi:10.2516/ogst/2009063

Devlin, J. F., Schillig, P. C., Bowen, I., Critchley, C. E., Rudolph, D. L., Thomson, N. R., … Roberts, J. a. (2012). Applications and implications of direct groundwater velocity measurement at the centimetre scale. *Journal of Contaminant Hydrology*, *127*(1-4), 3–14. doi:10.1016/j.jconhyd.2011.06.007

Doughty, C., Long, J. C. S., Hestir, K., & Benson, S. M. (1994). Hydrologic characterization of heterogeneous geologic media with an inverse method based on iterated function systems. *Water Resources Research*, *30*(6), 1721–1745.

Faybishenko, B., Witherspoon, P. A., & Benson, S. M. (Eds.). (2000). *Dynamics of fluids in fractured rock* (pp. 1–400). American Geophysical Union. doi:10.1029/GM122

Fossen, H. (Ed.). (2010). *Structural geology*. Cambridge University Press.

Irsa, J., & Zhang, Y. (2012). A direct method of parameter estimation for steady state flow in heterogeneous aquifers with unknown boundary conditions. *Water Resources Research*, *48*(9), n/a–n/a. doi:10.1029/2011WR011756

Kleinecke, D. (1971). Use of linear programing for estimating geohydrologic parameters of groundwater basins. *Water Resources Research*, *7*(2), 367–374.

Kowalsky, M. B., Finsterle, S., Williams, K. H., Murray, C., Commer, M., Newcomer, D., … Hubbard, S. S. (2012). On parameterization of the inverse problem for estimating aquifer

properties using tracer data. *Water Resources Research*, *48*(6), W06535. doi:10.1029/2011WR011203

Labaky, W., Devlin, J. F., & Gillham, R. W. (2009). Field comparison of the point velocity probe with other groundwater velocity measurement methods. *Water Resources Research*, *45*(4), n/a–n/a. doi:10.1029/2008WR007066

Lemonnier, P., & Bourbiaux, B. (2010). Simulation of naturally fractured reservoirs: state of the art. *Oil & Gas Science and Technology – Revue de l'Institut Français Du Pétrole*, *65*(2), 239–262. doi:10.2516/ogst/2009066

Mclaughlin, D., & Townley, L. R. (1996). A reassessment of the groundwater inverse problem. *Water Resources Research*, *32*(5), 1131–1161.

Moore, C., & Doherty, J. (2006). *The cost of uniqueness in groundwater model calibration. Advances in Water Resources* (Vol. 29, pp. 605–623). doi:10.1016/j.advwatres.2005.07.003

Nelson, R. W. (1960). In-place measurement of permeability in heterogeneous media: 1. Theory of a proposed method. *J. Geophys. Res.*, *65*(5), 1753–1760. doi:10.1029/JZ065i006p01753

Nelson, R. W. (1961). In-place measurement of permeability in heterogeneous media: 2. Experimental and computational considerations. *J. Geophys. Res.*, *66*(8), 2469–2478. doi:10.1029/JZ066i008p02469

Nelson, R. W. (1968). In-place determination of permeability distribution for heterogeneous porous media through analysis of energy dissipation. *Soc. Pet. Eng. J.*, *3*, 33–42.

Neuman, S. P. (1973). calibration of distributed parameter groundwater flow models viewed as a multiple objective decision process under uncertainty. *Water Resources Research*, *9*(4), 1006–1021.

Neuman, S. P. (2005). Trends, prospects and challenges in quantifying flow and transport through fractured rocks. *Hydrogeology Journal*, *13*(1), 124–147. doi:10.1007/s10040-004-0397-2

Perrodon, A. (1980). *Géodynamique pétrolière genèse et répartition des gisements d'hydrocarbures* (pp. 1–381). Elf Aquitaine.

Sagar, B., Yakowitz, S., & Duckstein, L. (1975). A direct method for the identification of the parameters of dynamic nonhomogeneous aquifers. *Water Resources Research*, *11*(4).

Sun, N.-Z. (1994). Inverse problems in groundwater modeling. Theory and applications of transport in porous media, vol. 6 (pp. 1–338). Kluwer Academic, Dordrecht, Netherlands.

Tiab, D., & Donaldson, E. C. (Eds.). (2011). *Petrophysics: theory and practice of measuring reservoir rock and fluid transport properties* (3rd ed., pp. 1–976). Gulf professional publishing.

Tsang, C., & Neretnieks, I. (1998). Flow channeling in heterogeneous fractured rocks. *Reviews of Geophysics*, *36*(2), 275–298.

Yeh, W. W.-G., Yoon, Y. S., & Lee, K. S. (1983). Aquifer parameter identification with kriging and optimum parameterization. *Water Resources Research*, *19*(1), 225–233.

Zhang, Y., Gable, C. W., & Person, M. (2006). Equivalent hydraulic conductivity of an experimental stratigraphy: Implications for basin-scale flow simulations. *Water Resources Research*, *42*(5), n/a–n/a. doi:10.1029/2005WR004720